cmgh
CELLULAR AND MOLECULAR GASTROENTEROLOGY AND HEPATOLOGY

ORIGINAL RESEARCH

Trypsin-Mediated Sensitization to Ferroptosis Increases the Severity of Pancreatitis in Mice

Ke Liu,[1] Jiao Liu,[2] Borong Zou,[2] Changfeng Li,[3] Herbert J. Zeh,[4] Rui Kang,[4] Guido Kroemer,[5,6,7] Jun Huang,[8] and Daolin Tang[4]

[1]Department of Ophthalmology, The 2nd Xiangya Hospital, Central South University, Changsha, China; [2]The Third Affiliated Hospital of Guangzhou Medical University, Guangzhou, Guangdong, China; [3]Department of Endoscopy Center, China–Japan Union Hospital of Jilin University, Changchun, Jilin, China; [4]Department of Surgery, University of Texas Southwestern Medical Center, Dallas, Texas; [5]Centre de Recherche des Cordeliers, Equipe Labellisée par la Ligue Contre le Cancer, Université de Paris, Sorbonne Université, INSERM U1138, Institut Universitaire de France, Paris, France; [6]Metabolomics and Cell Biology Platforms, Gustave Roussy Cancer Campus, Villejuif, France; [7]Pôle de Biologie, Hôpital Européen Georges Pompidou, AP-HP, Paris, France; [8]Department of Orthopaedics, The 2nd Xiangya Hospital, Central South University, Changsha, China

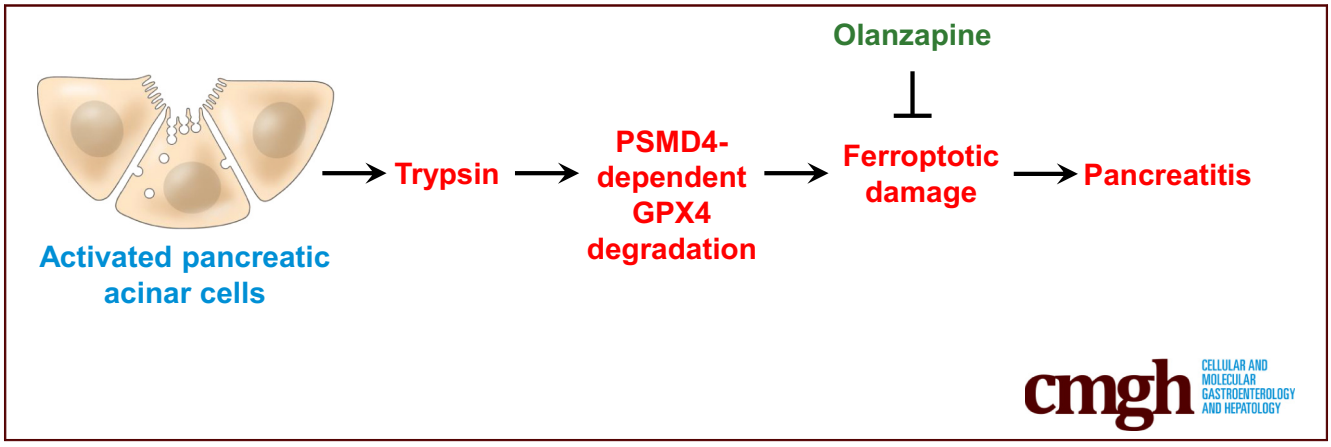

SUMMARY

Trypsin-mediated sensitization of pancreatic acinar cells to ferroptosis may be targeted for the prevention and treatment of pancreatitis in mice. An unbiased drug screening campaign identified olanzapine as a novel ferroptosis inhibitor that prevents pancreatitis in mice.

BACKGROUND & AIMS: Pancreatitis is characterized by acinar cell death and persistent inflammation. Ferroptosis is a type of lipid peroxidation-dependent necrosis, which is negatively regulated by glutathione peroxidase 4. We studied how trypsin, a serine protease secreted by pancreatic acinar cells, affects the contribution of ferroptosis to triggering pancreatitis.

METHODS: In vitro, the mouse pancreatic acinar cell line 266-6 and mouse primary pancreatic acinar cells were used to investigate the effect of exogenous trypsin on ferroptosis sensitivity. Short hairpin RNAs were designed to silence gene expression, whereas a library of 1080 approved drugs was used to identify new ferroptosis inhibitors in 266-6 cells. In vivo, a Cre/LoxP system was used to generate mice with a pancreas-specific knockout of *Gpx4* (*Pdx1-Cre;Gpx4*$^{flox/flox}$ mice). Acute or chronic pancreatitis was induced in these mice (*Gpx4*$^{flox/flox}$ mice served as controls) by cerulein injections or a Lieber–DeCarli alcoholic liquid diet. Pancreatic tissues, acinar cells, and serum were collected and analyzed by histology, immunoblot, quantitative polymerase chain reaction, enzyme-linked immunosorbent assay, or immunohistochemical analyses.

RESULTS: Supraphysiological doses of trypsin (500 or 1000 ng/mL) alone did not trigger significant cell death in 266-6 cells and mouse primary pancreatic acinar cells, but did increase the sensitivity of these cells to ferroptosis upon treatment with cerulein, L-arginine, alcohol, erastin, or RSL3. Proteasome 26S subunit, non–adenosine triphosphatase 4–dependent lipid peroxidation caused ferroptosis in pancreatic acinar cells by promoting the proteasomal degradation of glutathione peroxidase 4. The drug screening campaign identified the antipsychotic drug olanzapine as an antioxidant inhibiting ferroptosis in pancreatic acinar cells. Mice lacking pancreatic *Gpx4* developed more severe pancreatitis after cerulein infection or ethanol feeding than control mice. Conversely, olanzapine administration protected against pancreatic ferroptotic damage and experimental pancreatitis in *Gpx4*-deficient mice.

CONCLUSIONS: Trypsin-mediated sensitization to ferroptotic damage increases the severity of pancreatitis in mice, and this process can be reversed by olanzapine. *(Cell Mol Gastroenterol Hepatol 2022;13:483–500; https://doi.org/10.1016/j.jcmgh.2021.09.008)*

Keywords: Acinar Cells; Animal Model; Cell Death; Digestive Enzyme; Sterile Inflammation.

Pancreatitis is a progressive inflammatory disease caused by premature activation of digestive enzymes, such as trypsin.[1–3] Trypsin is normally produced in pancreatic acinar cells in a latent, inactive form (also known as trypsinogen), and is activated only in the lumen of the small intestine to digest proteins. The premature activation and release of trypsin may contribute to the pathogenesis of pancreatitis, as indicated by several lines of evidence. First, the levels of trypsin in serum or urine correlate with the severity of human pancreatitis.[4,5] Second, mutations affecting genes in the trypsin activation (eg, *PRSS1* and *SPINK1*) are implicated in human pancreatitis.[6–12] Third, transgenic expression of human *PRSS1* mutations in mice results in a phenotype that is highly susceptible to experimental pancreatitis.[13–15] Fourth, the activation of trypsinogen resulting in excessive trypsin production can cause pancreatic acinar cell damage and/or activate immune pathways (such as nuclear factor-κB) to trigger pancreatitis in mice.[16–20] However, despite the introduction of this trypsin paradigm for almost 40 years, the mechanism of action of trypsin in pancreatitis still is elusive.[21]

The pathogenesis of pancreatitis involves the excessive induction of multiple distinct cell death pathways.[22,23] The severity of pancreatitis is tightly related to necrosis.[24,25] Ferroptosis is a type of regulated necrosis driven by iron-dependent lipid peroxidation and subsequent plasma membrane rupture.[26,27] Excessive ferroptotic cell death causes sterile inflammation through the release of endogenous damage-associated molecular patterns.[28] Although it is well established that iron metabolism is altered in pancreatitis,[29] the contribution of iron-dependent ferroptotic damage to pancreatitis still is poorly understood.[30–32] Here, we investigated the previously elusive relationship between trypsin and ferroptosis during the progression of experimental pancreatitis. Using a combination of drug screening experiments and conditional knockout mouse models, we found that trypsin can enhance ferroptotic death in acinar cells, thus exacerbating pancreatitis. Our results suggest that trypsin-mediated ferroptotic death might constitute a therapeutic target for mitigating pancreatitis.

Results

Trypsin Increases the Sensitivity of Pancreatic Acinar Cells to Ferroptosis

In patients with acute pancreatitis or in the acute phase of chronic pancreatitis, serum trypsin levels reportedly increase to 500–1000 ng/mL.[33,34] To determine the effects of trypsin on cell death, we treated the mouse pancreatic acinar cell line 266-6 and mouse primary pancreatic acinar cells (mPACs) with cell culture–grade trypsin, which was devoid of endotoxin or other biological contaminants. Trypsin used in the reported pathogenic range (500 or 1000 ng/mL) did not trigger significant cell death in 266-6 cells and mPACs, but higher doses (>1000 ng/mL) resulted in cell killing (Figure 1*A*). Next, we exposed 266-6 cells and mPACs to pancreatitis-inducing toxins, including cerulein, L-arginine, or alcohol, in the absence or presence of trypsin (500 ng/mL). Of note, trypsin increased the sensitivity of acinar cells to cell death induction by these pancreatitis-related stimuli, while a widely used trypsin inhibitor, namely soybean trypsin inhibitor (STI),[35] reduced cell killing by cerulein, L-arginine, or alcohol (Figure 1*B*). These findings indicate that trypsin sensitizes pancreatic acinar cells to cell death.

To elucidate the mechanism of trypsin-enhanced acinar cell death, we monitored the levels of oxidative stress by means of the quantitation of malondialdehyde (MDA), a product of lipid peroxidation.[36] Cerulein-, L-arginine-, or alcohol-induced MDA production was increased by addition of trypsin to the cell culture (Figure 1*C*). This increased MDA production was blocked by addition of the trypsin inhibitor STI (Figure 1*C*). Of note, trypsin-mediated cell death sensitivity and MDA production were completely reverted by ferroptosis inhibitors (eg, ferrostatin-1, liproxstatin-1, or 2-mercaptoethanol),[37] but not by inhibitors of apoptosis (eg, Z-VAD-FMK) or necroptosis (eg, necrosulfonamide) (Figure 1*B* and *C*). As a positive control, Z-VAD-FMK or necrosulfonamide inhibited cell death initiated by staurosporine (an apoptosis inducer[38]) or CCT137690 (a necroptosis inducer[39]) in 266-6 cells and mPACs, respectively (Figure 1*D*). Trypsin enhanced the cell death and MDA production triggered by classic ferroptosis inducers (eg, erastin or RSL3)[37] in 266-6 cells or mPACs, and these processes were blocked by ferrostatin-1, liproxstatin-1, 2-mercaptoethanol, or STI (Figure 1*B* and *C*). Altogether, these results indicate that the presence of trypsin sensitizes pancreatic acinar cells to the induction of ferroptosis.

Proteasome 26S Subunit, Non–Adenosine Triphosphatase 4–Dependent Lipid Peroxidation Promotes Ferroptosis in Acinar Cells

The proteasome is a large protein complex composed of 43 different subunits, which are jointly responsible for the selective degradation of proteins by proteolysis. The proteasome plays a dual (inhibitory or facilitatory) role in ferroptosis, depending on the specific substrate protein involved in the process.[40–43] To define the core components

Abbreviations used in this paper: **ACSL4, acyl-CoA synthetase long chain family member 4; ARNTL, aryl hydrocarbon receptor nuclear translocator-like; cDNA, complementary DNA; CoQ10, coenzyme Q10; DPPH, 2,2-diphenyl-1-picrylhydrazyl; GPX4, glutathione peroxidase 4; GSH, glutathione; HMGB1, high mobility group box 1; IL, interleukin; IL1B, interleukin 1β; KO, knockout; LDH, lactate dehydrogenase; MDA, malondialdehyde; mPAC, mouse primary pancreatic acinar cell; MPO, myeloperoxidase; mRNA, messenger RNA; p-MLKL, phosphorylated mixed-lineage kinase domain-like pseudokinase; PSMD4, proteasome 26S subunit, non–adenosine triphosphatase 4; PTGS2, prostaglandin-endoperoxide synthase 2; qPCR, quantitative polymerase chain reaction; shRNA, short hairpin RNA; SLC40A1, solute carrier family 40 member 1; STI, soybean trypsin inhibitor; TBST, Tris-buffered saline with 0.1% Tween 20 detergent; WT, wild-type.**

Most current article

2352-345X
https://doi.org/10.1016/j.jcmgh.2021.09.008

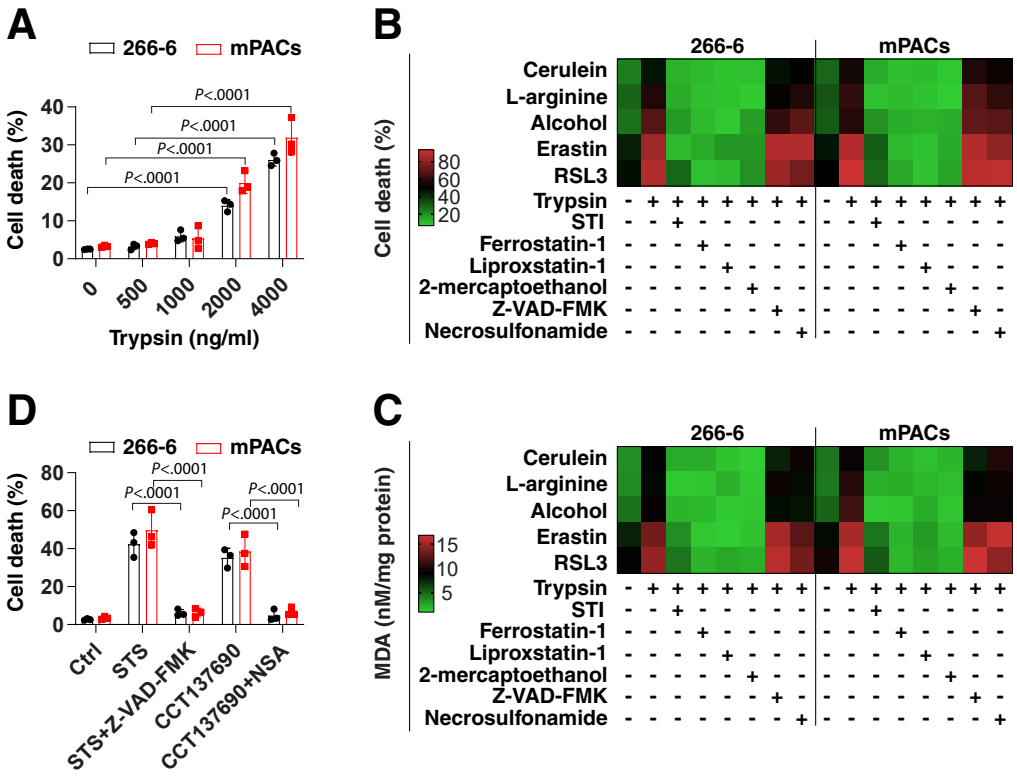

Figure 1. Trypsin increases the sensitivity of pancreatic acinar cells to ferroptosis. (*A*) Analysis of cell death in indicated acinar cells after treatment with trypsin (500–4000 ng/mL) for 24 hours. Data are presented as means ± SD; n = 3 biologically independent samples; 2-way analysis of variance with the Tukey multiple comparisons test on all pairwise combinations. (*B* and *C*) Analysis of cell death and MDA in indicated acinar cells after treatment with cerulein (100 nmol/L), L-arginine (5 mg/mL), alcohol (50 mmol/L), erastin (2 μmol/L), and RSL3 (500 nmol/L) in the absence or presence of trypsin (500 ng/mL), STI (500 ng/mL), ferrostatin-1 (1 μmol/L), liproxstatin-1 (500 nmol/L), 2-mercaptoethanol (20 μmol/L), Z-VAD-FMK (10 μmol/L), or necrosulfonamide (1 μmol/L) for 24 hours. Data are shown in a heat map as the mean of 3 biologically independent samples. (*D*) Analysis of cell death in indicated acinar cells after treatment with staurosporine (STS, 500 nmol/L) or CCT137690 (1 μmol/L) in the absence or presence of Z-VAD-FMK (10 μmol/L) or necrosulfonamide (NSA, 1 μmol/L) for 24 hours. Data are presented as means ± SD; n = 3 biologically independent samples; 2-way analysis of variance with the Tukey multiple comparisons test on all pairwise combinations. Ctrl, control.

of the proteasome responsible for ferroptosis modulation in acinar cells, we used quantitative polymerase chain reaction (qPCR) to measure the levels of messenger RNAs (mRNAs) coding for the 43 proteasome subunits in 266-6 cells treated with cerulein alone or together with trypsin. The proteasome 26S subunit, non–adenosine triphosphatase 4 (*Psmd4*) ranked as the most up-regulated gene in 266-6 cells after treatment with cerulein plus trypsin (Figure 2*A*). In contrast, cerulein or trypsin alone did not cause significant up-regulation of *Psmd4* mRNA in 266-6 cells and mPACs (Figure 2*B*).

To determine whether the proteasome 26S subunit, non–adenosine triphosphatase 4 (PSMD4) is involved in ferroptosis, we suppressed *Psmd4* expression by specific short hairpin RNAs (shRNAs) (Figure 2*C*). In the presence of trypsin, the knockdown of *Psmd4* limited the death of 266-6 cells caused by cerulein, L-arginine, alcohol, erastin, or RSL3 (Figure 2*D*). In contrast, transfection-enforced overexpression of *Psmd4* (Figure 2*C*) restored the sensitivity of *Psmd4*-depleted 266-6 cells to these ferroptosis inducers (Figure 2*D*), confirming that PSMD4 is a positive regulator of ferroptosis in acinar cells.

Lipid peroxidation plays a major role in promoting ferroptosis owing to its implication in membrane damage as well as in DNA damage.[44] Oxidized phosphatidylethanolamine-polyunsaturated fatty acids, such as arachidonic acid (C20:4) and adrenic acid (C22:4), play a direct role in promoting ferroptosis.[45] We examined the effects of PSMD4 on the production of lipid peroxidation products, including MDA (Figure 2*E*), 8-hydroxy-2-deoxyguanosine (a product of oxidative DNA damage) (Figure 2*F*), C20:4 (Figure 2*G*), and C22:4 (Figure 2*H*). Of note, *Psmd4* depletion blocked the generation of these lipid peroxidation products in 266-6 cells after treatment with cerulein, L-arginine, alcohol, erastin, or RSL3 in the presence of trypsin (Figure 2*E–H*). The measurement of lipid peroxidation products by means of the boron dipyrromethene difluoride (BODIPY) 581/591 C11 assay confirmed the decrease in oxidative reactions in *Psmd4*-knockdown 266-6 cells (Figure 2*I*). In contrast, *Psmd4* knockdown failed to affect staurosporine- or CCT137690-induced cell death (Figure 2*J*). Moreover, cell death induced by erastin or RSL3 alone was not influenced by

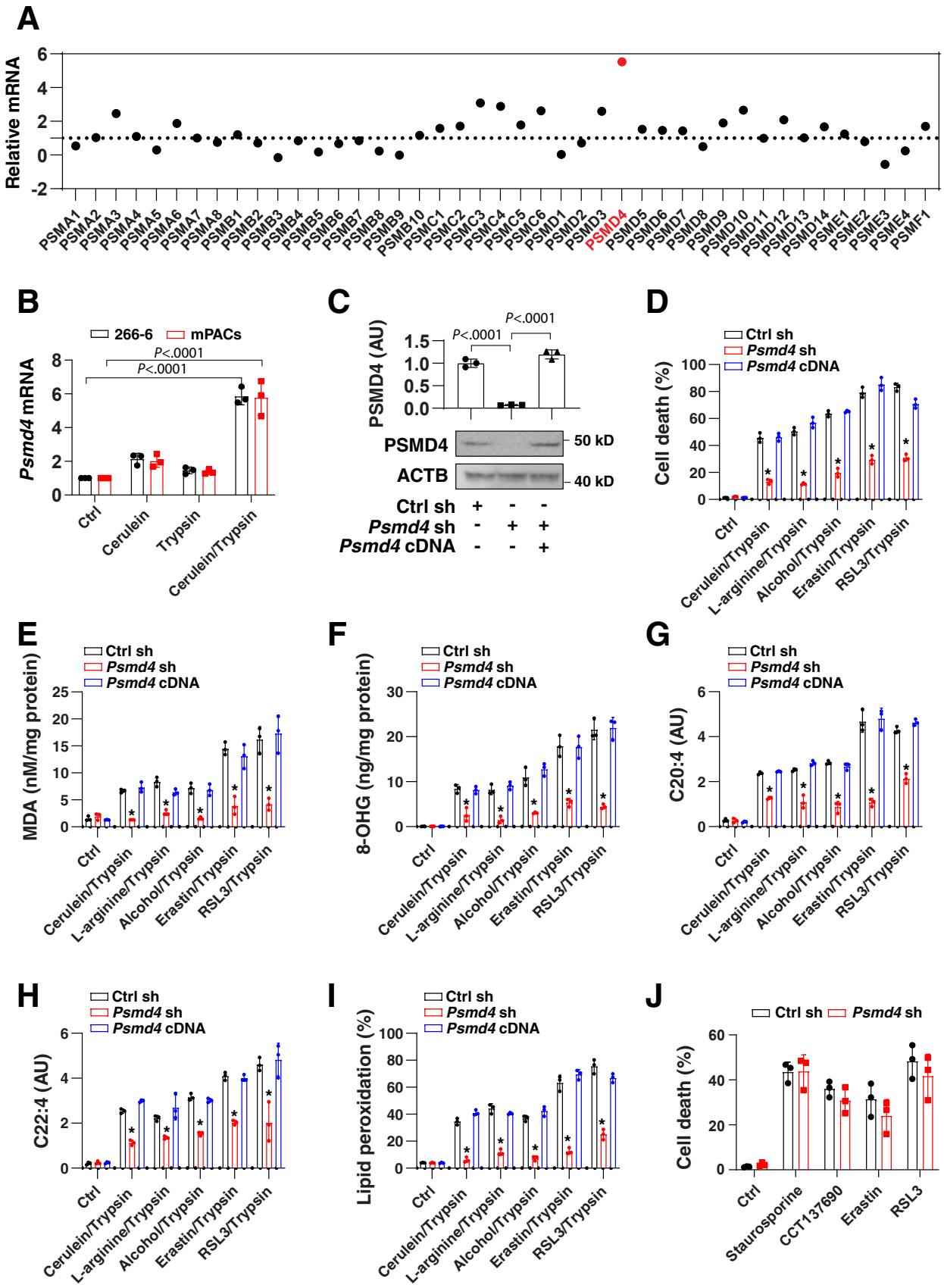
A
Relative mRNA
PSMA1 PSMA2 PSMA3 PSMA4 PSMA5 PSMA6 PSMA7 PSMA8 PSMB1 PSMB2 PSMB3 PSMB4 PSMB5 PSMB6 PSMB7 PSMB8 PSMB9 PSMB10 PSMC1 PSMC2 PSMC3 PSMC4 PSMC5 PSMC6 PSMD1 PSMD2 PSMD3 PSMD4 PSMD5 PSMD6 PSMD7 PSMD8 PSMD9 PSMD10 PSMD11 PSMD12 PSMD13 PSMD14 PSME1 PSME2 PSME3 PSME4 PSMF1
B
266-6 mPACs
Psmd4 mRNA
P<.0001
P<.0001
Ctrl Cerulein Trypsin Cerulein/Trypsin
C
PSMD4 (AU)
P<.0001
P<.0001
PSMD4
ACTB
50 kD
40 kD
Ctrl sh + - -
Psmd4 sh - + +
Psmd4 cDNA - - +
D
Ctrl sh
Psmd4 sh
Psmd4 cDNA
Cell death (%)
Ctrl Cerulein/Trypsin L-arginine/Trypsin Alcohol/Trypsin Erastin/Trypsin RSL3/Trypsin
E
Ctrl sh
Psmd4 sh
Psmd4 cDNA
MDA (nM/mg protein)
Ctrl Cerulein/Trypsin L-arginine/Trypsin Alcohol/Trypsin Erastin/Trypsin RSL3/Trypsin
F
Ctrl sh
Psmd4 sh
Psmd4 cDNA
8-OHG (ng/mg protein)
Ctrl Cerulein/Trypsin L-arginine/Trypsin Alcohol/Trypsin Erastin/Trypsin RSL3/Trypsin
G
Ctrl sh
Psmd4 sh
Psmd4 cDNA
C20:4 (AU)
Ctrl Cerulein/Trypsin L-arginine/Trypsin Alcohol/Trypsin Erastin/Trypsin RSL3/Trypsin
H
Ctrl sh
Psmd4 sh
Psmd4 cDNA
C22:4 (AU)
Ctrl Cerulein/Trypsin L-arginine/Trypsin Alcohol/Trypsin Erastin/Trypsin RSL3/Trypsin
I
Ctrl sh
Psmd4 sh
Psmd4 cDNA
Lipid peroxidation (%)
Ctrl Cerulein/Trypsin L-arginine/Trypsin Alcohol/Trypsin Erastin/Trypsin RSL3/Trypsin
J
Ctrl sh
Psmd4 sh
Cell death (%)
Ctrl Staurosporine CCT137690 Erastin RSL3

Psmd4 knockdown in 266-6 cells (Figure 2*J*). Altogether, these findings support the interpretation that PSMD4 selectively promotes trypsin-related ferroptosis by inducing lipid peroxidation.

PSMD4-Dependent Glutathione Peroxidase 4 Degradation Promotes Ferroptosis in Acinar Cells

Glutathione peroxidase 4 (GPX4) is a key antioxidant enzyme that detoxifies lipid peroxides during ferroptosis.[46,47] Accordingly, GPX4 degradation by proteasomes or autophagy favors the induction of ferroptosis.[42,48] Driven by these considerations, we determined whether PSMD4 might affect GPX4 degradation in acinar cells. Western blot and qPCR analysis showed that, after treatment with cerulein in the presence of trypsin, the protein levels of GPX4 (but not the mRNA levels of *Gpx4*) were reduced in control cells, but not in *Psmd4*-depleted 266-6 cells (Figure 3*A* and *B*). These results indicate that, in acinar cells, PSMD4 inhibits cerulein-/trypsin-induced down-regulation of GPX4 protein, but not *Gpx4* mRNA.

The selective autophagic degradation of the iron storage protein ferritin,[49] the circadian clock regulator aryl hydrocarbon receptor nuclear translocator-like (ARNTL, best known as brain and mMuscle ARNT-like 1 [BMAL1]),[50] and the iron export protein solute carrier family 40 member 1 (SLC40A1, also known as ferroportin-1)[51] all promote ferroptosis. However, the knockdown of *Psmd4* failed to affect the protein expression of ferritin heavy chain 1, ARNTL, and SLC40A1 during cerulein-/trypsin-induced ferroptosis (Figure 3*C*), indicating that PSMD4 is not required for autophagy-dependent ferroptosis.[51,52] Other important regulators of ferroptosis, such as apoptosis inducing factor mitochondria-associated 2 (an oxidoreductase involved in producing reduced coenzyme Q10 [CoQ10])[53–55] and SLC7A11 (a subunit of the cystine/glutamate antiporter system xc^- that promotes cystine uptake and glutathione [GSH] biosynthesis),[37] also remained unaffected by PSMD4 (Figure 3*C*). Accordingly, the knockdown of *Psmd4* failed to affect the intracellular levels of iron, GSH, and CoQ10, as well as the mRNA expression of *Egln2* (an ARNTL-targeted gene involved in ferroptosis[50]) in cerulein-/trypsin-treated 266-6 cells (Figure 3*D*–*G*).

In the early stages of the induction of ferroptosis by cerulein/trypsin, a protein complex containing PSMD4 and GPX4 was observed in 266-6 cells (Figure 3*H*). Functionally, the knockdown of *Gpx4* by shRNAs (Figure 3*I*) restored the sensitivity of *Psmd4*-depleted 266-6 cells to ferroptosis (Figure 3*J*), which was associated with increased lipid peroxidation (Figure 3*K*), C20:4 (Figure 3*L*), or C22:4 (Figure 3*M*). Altogether, these findings indicate that PSMD4-mediated GPX4 degradation promotes lipid peroxidation-mediated ferroptosis in pancreatic acinar cells.

Olanzapine Is a New Ferroptosis Inhibitor in Acinar Cells

Most ferroptosis inhibitors are experimental drugs (eg, ferrostatin-1 or liproxstatin-1), but have not been characterized yet in clinical trials.[56] Driven by this consideration, we screened a library of 1080 Food and Drug Administration–approved drugs for their capacity to inhibit ferroptosis caused by cerulein/trypsin in 266-6 cells. The top 5 compounds that blocked cerulein-/trypsin-induced cell death included olanzapine (an antipsychotic drug), idebenone (a synthetic analogue of CoQ10), telmisartan (an angiotensin II receptor blocker), nisoldipine (a calcium channel blocker), and azelnidipine (a dihydropyridine calcium channel blocker) (Figure 4*A*). These top 5 drugs were evaluated further in 266-6 cells or mPACs challenged with trypsin combined with cerulein, L-arginine, alcohol, erastin, or RSL. These results confirmed that olanzapine and idebenone can suppress ferroptosis in various conditions (Figure 4*B*). Given that CoQ10 already has been characterized as a ferroptosis inhibitor,[53,54] we focused on olanzapine in subsequent studies.

Although the mechanism of action of olanzapine is unknown, it has been proposed that its antipsychotic action involves the inhibition of serotonin type 2 (5-hydroxytryptamine 2) receptors, including HTR2A/5-HT2A, HTR2B/5-HT2B, and HTR2C/5-HT2C. Unlike olanzapine, selective antagonists of HTR2A (risperidone), HTR2B (SB204741), or HTR2C (SB242084) failed to inhibit cerulein-/trypsin-induced ferroptotic death in 266-6 cells or mPACs (Figure 4*C*), suggesting that olanzapine acts through off-target effects to block ferroptosis. Indeed, the knockdown of *Htr2a*, *Htr2b*,

Figure 2. (*See previous page*). PSMD4-dependent lipid peroxidation promotes ferroptosis in acinar cells. (*A*) Analysis of mRNA expression of 43 proteasome subunits in 266-6 cells after treatment with cerulein (100 nmol/L) in the presence of trypsin (500 ng/mL) for 24 hours. Data are shown in a scatter map as the mean of 3 biologically independent samples. *Psmd4* ranked as the most up-regulated gene as shown in red. (*B*) Analysis of mRNA expression of *Psmd4* in 266-6 cells and mPACs after treatment with cerulein (100 nmol/L) in the absence or presence of trypsin (500 ng/mL) for 24 hours. Data are presented as means ± SD; n = 3 biologically independent samples; 2-way analysis of variance (ANOVA) with the Tukey multiple comparisons test on all pairwise combinations. (*C*) Analysis of protein expression of PSMD4 in indicated 266-6 cells. Semiquantitative data are presented as means ± SD; n = 3 biologically independent samples; 1-way ANOVA test on all pairwise combinations. (*D–I*) Analysis of (*D*) cell death, (*E*) MDA, (*F*) 8-hydroxy-2-deoxyguanosine (8-OHG), (*G*) C20:4, (*H*) C22:4, or (*I*) lipid peroxidation in indicated 266-6 cells after treatment with cerulein (100 nmol/L), L-arginine (5 mg/mL), alcohol (50 mmol/L), erastin (2 μmol/L), and RSL3 (500 nmol/L) in the presence of trypsin (500 ng/mL) for 24 hours. Data are presented as mean ± SD; n = 3 biologically independent samples; 2-way ANOVA test on all pairwise combinations (*$P < .0001$ vs control shRNA group or *Psmd4* cDNA group). (*J*) Analysis of cell death in indicated 266-6 cells after treatment with staurosporine (500 nmol/L), CCT137690 (1 μmol/L), erastin (2 μmol/L), or RSL3 (500 nmol/L) in the absence of trypsin for 24 hours. Data are presented as means ± SD; n = 3 biologically independent samples; 2-way ANOVA with the Tukey multiple comparisons test on all pairwise combinations. Ctrl, control.

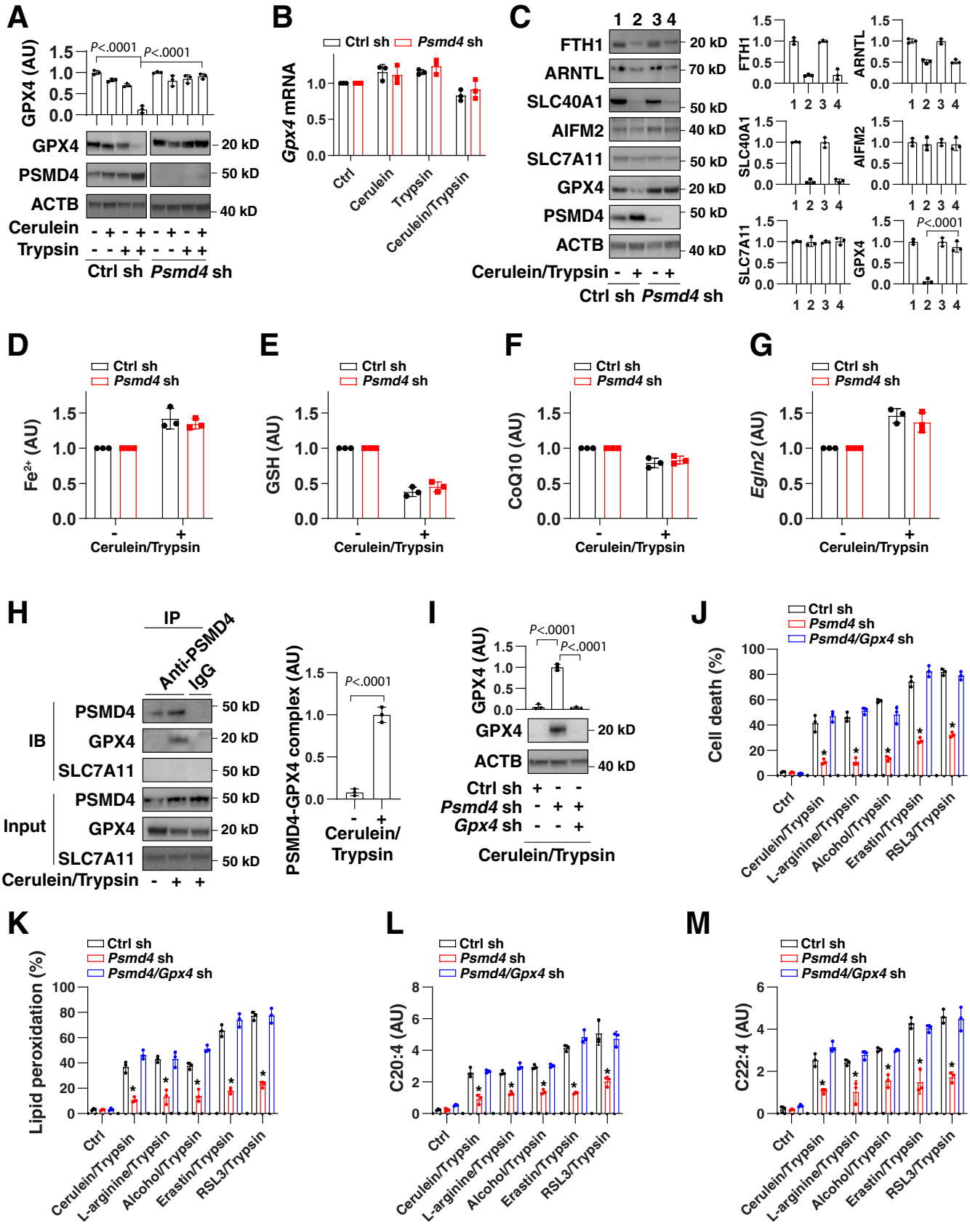
A
GPX4 (AU)
P<.0001
P<.0001
GPX4
PSMD4
ACTB
20 kD
50 kD
40 kD
Cerulein
Trypsin
Ctrl sh Psmd4 sh
B
Ctrl sh Psmd4 sh
Gpx4 mRNA
Ctrl
Cerulein
Trypsin
Cerulein/Trypsin
C
1 2 3 4
FTH1
ARNTL
SLC40A1
AIFM2
SLC7A11
GPX4
PSMD4
ACTB
20 kD
70 kD
50 kD
40 kD
Cerulein/Trypsin
Ctrl sh Psmd4 sh
P<.0001
D
Ctrl sh
Psmd4 sh
Fe2+ (AU)
Cerulein/Trypsin
E
GSH (AU)
F
CoQ10 (AU)
G
Egln2 (AU)
H
IP
Anti-PSMD4
IgG
IB
Input
PSMD4
GPX4
SLC7A11
50 kD
20 kD
Cerulein/Trypsin
PSMD4-GPX4 complex (AU)
Cerulein/
Trypsin
I
GPX4 (AU)
Ctrl sh
Psmd4 sh
Gpx4 sh
Cerulein/Trypsin
J
Psmd4/Gpx4 sh
Cell death (%)
Ctrl
Cerulein/Trypsin
L-arginine/Trypsin
Alcohol/Trypsin
Erastin/Trypsin
RSL3/Trypsin
K
Lipid peroxidation (%)
L
C20:4 (AU)
M
C22:4 (AU)

and *Htr2c* by shRNAs also failed to affect cerulein-/trypsin-induced cell death in 266-6 cells (Figure 4*D* and *E*). As a positive control, the knockdown of ferroptotic promoter *Acsl4*[45,57,58] inhibited cerulein-/trypsin-induced cell death in 266-6 cells (Figure 4*D* and *E*).

We used the 2,2-diphenyl-1-picrylhydrazyl (DPPH) free radical scavenging assay in a cell-free system to determine whether the off-target activity of olanzapine involves antioxidant effects. Similar to ferrostatin-1 (positive control), the olanzapine-mediated suppression of ferroptosis correlated with its antioxidant activity (Figure 4*F*). In contrast, the 5-hydroxytryptamine 2 antagonists (risperidone, SB204741, and SB242084) failed to show such antioxidant effects (Figure 4*F*). Moreover, olanzapine inhibited cerulein-/trypsin-induced lipid peroxidation (Figure 4*G*), C20:4 (Figure 4*H*), and C22:4 (Figure 4*I*). In contrast, olanzapine had no significant impact on cerulein-/trypsin-induced GPX4 degradation in 266-6 cells (Figure 4*J*). Collectively, these data suggest that olanzapine protects against ferroptotic cell death through antioxidant effects.

Ferroptotic Damage Increases the Severity of Acute Pancreatitis in Mice

We recently showed that the conditional knockout (KO) of *Gpx4* within the pancreas of mice (termed KO mice) accelerated cerulein-induced acute pancreatitis by ferroptotic damage.[32] We used this model to evaluate whether olanzapine protects against ferroptosis-induced acute pancreatitis. Histologic assessment of pancreatic damage showed exaggerated acinar cell death, leukocyte infiltration, and interstitial edema in the KO mice compared with control mice (termed wild-type [WT] mice) (Figure 5*A*). These histologic changes were accompanied by significantly increased levels of pancreatitis parameters, including the activation of the endoplasmic reticulum stress signaling pathway (as measured by mRNA expression of pancreatic heat shock protein family A member 5 [*Hspa5*, also known as *Bip* or *Grp78*]) (Figure 5*B*), serum amylase (Figure 5*C*), pancreatic trypsin activity (Figure 5*D*), pancreatic neutrophil recruitment (as measured by pancreatic myeloperoxidase [MPO] activity) (Figure 5*E*), pancreatic necrosis (as reflected by serum lactate dehydrogenase [LDH] and high mobility group box 1 [HMGB1]) (Figure 5*F* and *G*, respectively), and serum trypsin activity (Figure 5*H*). The pancreatic expression of biomarkers of ferroptosis (eg, *Ptgs2* and *Acsl4*) (Figure 5*I* and *J*, respectively), but not biomarkers of apoptosis (eg, cleaved caspase-3) (Figure 5*K*) and necroptosis (eg, phosphorylated mixed-lineage kinase domain-like pseudokinase [p-MLKL]) (Figure 5*L*), were increased in cerulein-treated KO mice. As expected, the level of pancreatic MDA was increased in cerulein-treated KO mice (Figure 5*M*). The administration of olanzapine protected against all features of cerulein-induced acute pancreatitis in mice (especially KO mice), meaning that it prevented pancreatic dysfunction, tissue injury, inflammation, ferroptosis, and MDA production (Figure 5).

Ferroptotic Damage Accelerates the Development of Chronic Pancreatitis in Mice

Epidemiologic studies have shown that high alcohol consumption is associated with an increased risk of pancreatitis.[59] To further determine the interaction between ferroptosis and clinically relevant environmental insults, we first assessed the effects of pancreatic *Gpx4* deletion on chronic pancreatitis initiated by a Lieber–DeCarli alcoholic liquid diet. Ethanol feeding caused histologic changes in the pancreas in 15% (3 of 20) of WT mice (Figure 6*A*). In contrast, ethanol feeding led to the development of chronic inflammatory changes and pancreatic tissue injury in 85% (17 of 20) of KO mice (Figure 6*A*). Pancreatic fibrosis, a feature of chronic pancreatitis, also was increased in KO mice (Figure 6*A*). Accordingly, serum amylase, LDH, HMGB1, pancreatic MPO and trypsin activity, serum trypsin activity, pancreatic *Ptgs2* and *Acsl4* mRNA expression, as well as serum cytokines (tumor necrosis factor, interleukin 6 [IL6], and IL1β [IL1B]) were increased in KO mice compared with WT mice (Figure 6*B*–*M*). This *Gpx4* depletion-mediated chronic pancreatitis response was blocked by olanzapine, further supporting the hypothesis that ferroptotic damage promotes the development of chronic pancreatitis. As a control, *Gpx4* depletion and olanzapine had no effects on biomarkers of apoptosis

Figure 3. (***See previous page***). **PSMD4-dependent GPX4 degradation promotes ferroptosis in acinar cells.** (*A* and *B*) Analysis of (*A*) protein or (*B*) mRNA expression of GPX4 in control or *Psmd4*-knockdown 266-6 cells after treatment with cerulein (100 nmol/L) in the absence or presence of trypsin (500 ng/mL) for 24 hours. Data for mRNA are presented as means ± SD; n = 3 biologically independent samples. Two-way analysis of variance (ANOVA) test on all pairwise combinations. (*C*–*G*) Analysis of (*C*) protein expression, (*D*) intracellular Fe^{2+}, (*E*) intracellular GSH, (*F*) intracellular CoQ10, and (*G*) *Egln2* mRNA in control or *Psmd4*-knockdown 266-6 cells after treatment with cerulein (100 nmol/L) in the presence of trypsin (500 ng/mL) for 24 hours. Data are presented as means ± SD; n = 3 biologically independent samples. One-way ANOVA test on all pairwise combinations. (*H*) Immunoprecipitation (IP) analysis of the interaction between PSMD4 and GPX4 in 266-6 cells after treatment with cerulein (100 nmol/L) in the presence of trypsin (500 ng/mL) for 6 hours. Semiquantitative data are presented as means ± SD; n = 3 biologically independent samples; *t* test. (*I*) Analysis of protein expression in indicated 266-6 cells after treatment with cerulein (100 nmol/L) in the presence of trypsin (500 ng/mL) for 24 hours. Semiquantitative data are presented as means ± SD; n = 3 biologically independent samples; 1-way ANOVA test on all pairwise combinations. (*J*–*M*) Analysis of (*J*) cell death, (*K*) lipid peroxidation, (*L*) C20:4, or (*M*) C22:4 in indicated 266-6 cells after treatment with cerulein (100 nmol/L), L-arginine (5 mg/mL), alcohol (50 mmol/L), erastin (2 μmol/L), and RSL3 (500 nmol/L) in the presence of trypsin (500 ng/mL) for 24 hours. Data are presented as means ± SD; n = 3 biologically independent samples; 2-way ANOVA test on all pairwise combinations. *$P < .0001$ vs control sh or *Psmd4/Gpx4* sh group. ACTB, actin beta; Ctrl, control; IB, immunoblotting; sh, shRNA.

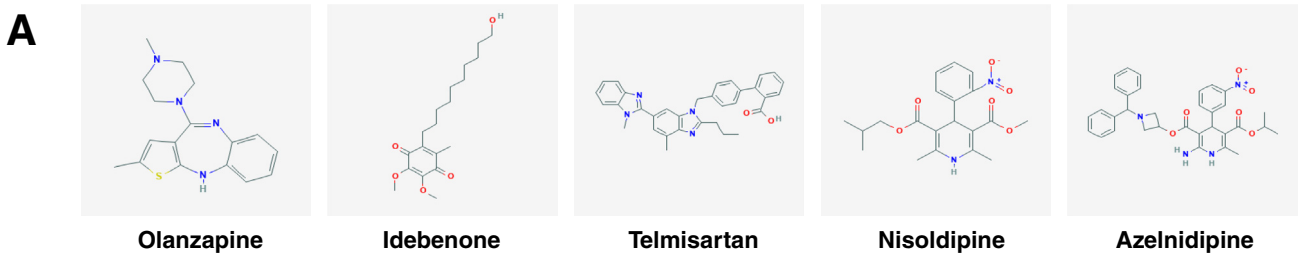
A
Olanzapine
Idebenone
Telmisartan
Nisoldipine
Azelnidipine

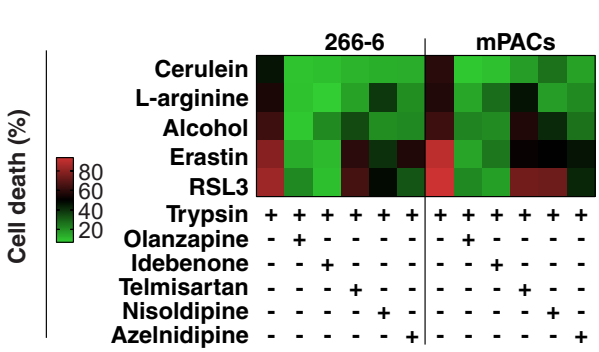
B
266-6
mPACs
Cell death (%)
80
60
40
20
Cerulein
L-arginine
Alcohol
Erastin
RSL3
Trypsin
Olanzapine
Idebenone
Telmisartan
Nisoldipine
Azelnidipine

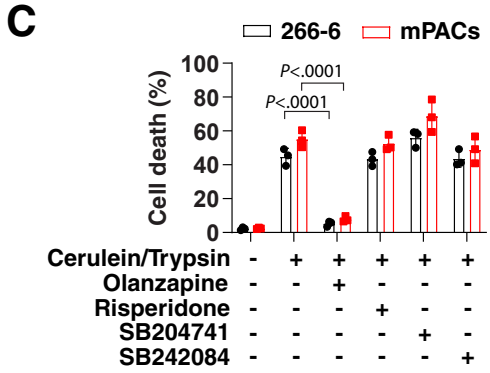
C
266-6
mPACs
Cell death (%)
P<.0001
P<.0001
Cerulein/Trypsin
Olanzapine
Risperidone
SB204741
SB242084

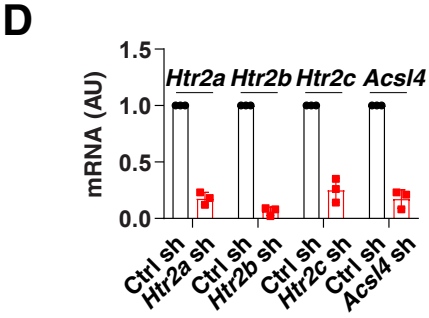
D
mRNA (AU)
Htr2a Htr2b Htr2c Acsl4
Ctrl sh
Htr2a sh
Htr2b sh
Htr2c sh
Acsl4 sh

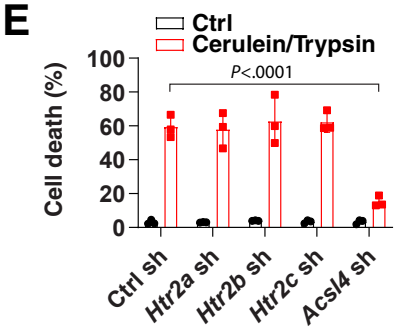
E
Ctrl
Cerulein/Trypsin
Cell death (%)
P<.0001
Ctrl sh
Htr2a sh
Htr2b sh
Htr2c sh
Acsl4 sh

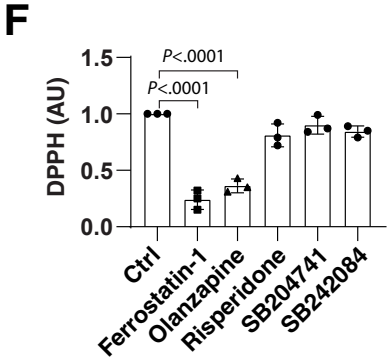
F
DPPH (AU)
P<.0001
P<.0001
Ctrl
Ferrostatin-1
Olanzapine
Risperidone
SB204741
SB242084

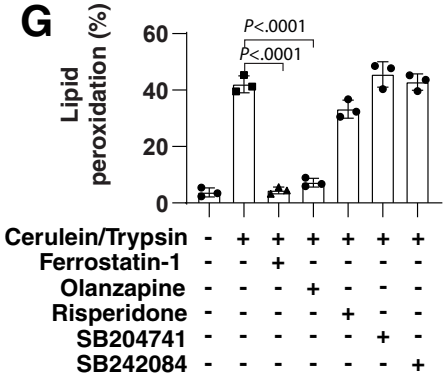
G
Lipid peroxidation (%)
P<.0001
P<.0001
Cerulein/Trypsin
Ferrostatin-1
Olanzapine
Risperidone
SB204741
SB242084

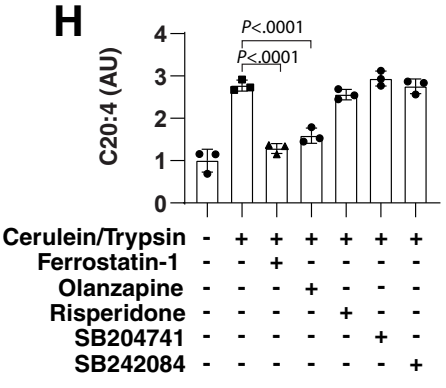
H
C20:4 (AU)
P<.0001
P<.0001
Cerulein/Trypsin
Ferrostatin-1
Olanzapine
Risperidone
SB204741
SB242084

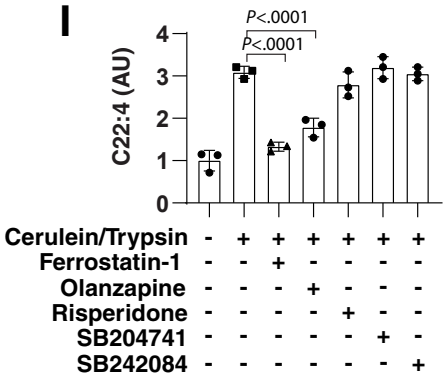
I
C22:4 (AU)
P<.0001
P<.0001
Cerulein/Trypsin
Ferrostatin-1
Olanzapine
Risperidone
SB204741
SB242084

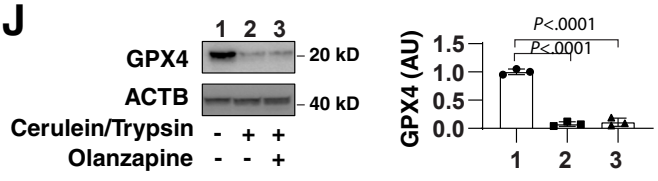
J
1 2 3
GPX4
20 kD
ACTB
40 kD
Cerulein/Trypsin
Olanzapine
GPX4 (AU)
P<.0001
P<.0001

(cleaved caspase-3) or necroptosis (p-MLKL) (Figure 6*N* and *O*).

Discussion

Understanding the mechanisms and functions of pancreatic necrosis is essential for the development of pancreatitis treatment strategies.[22] In this study, we reported a role for extracellular trypsin in the sensitization of acinar cells to ferroptotic death by inducing PSMD4-dependent GPX4 degradation. We further showed that, in experimental models of acute or chronic pancreatitis, olanzapine inhibits ferroptosis, improves pancreatic function, blunts inflammation, and limits tissue damage in pancreatic *Gpx4* KO mice. These findings enhance our understanding of the pathologic link between abnormal digestive enzyme changes and tissue damage in pancreatitis.

Although many endogenous factors or exogenous factors affect the function of the pancreas, the activation and secretion of digestive enzymes is considered to be one of the important initial signals of pancreatitis.[60] For example, the activation of trypsin occurs early in the disease process, parallel to organ damage and inflammation.[4,5] Mechanistically, the proteolytic activation of trypsin from trypsinogen (the precursor of trypsin) requires cathepsin B,[61] and pharmacologic or genetic blockade of cathepsin B prevents pancreatitis in mice.[61,62] Cathepsin B is also a mediator of ferroptosis.[63,64] These findings suggest an important role for lysosomal hydrolases in both trypsin activation and ferroptosis.

Although early studies using genetic mouse models that express R122H or p.D23A trypsinogen suggested that trypsin activation alone may directly cause pancreatitis,[65,66] recent studies using genetic mouse models that express human wild-type *PRSS1* (which encodes cationic trypsinogen) or its mutant form (R122H or K23R) have shown that trypsin activation is not sufficient to induce spontaneous pancreatitis.[13–15,67] In contrast, serine protease 1 mice are more sensitive to experimental pancreatitis induced by cerulein, ethanol, or a high-fat diet,[13–15,67] indicating that trypsin needs to be combined with other risk factors to induce pancreatitis. Our current study provides a theoretical model to suggest that active trypsin increases the risk of pancreatitis caused by ferroptotic damage.

Trypsin has enzyme digestion–dependent and –independent functions, relying on its concentration. In addition to extracellular trypsin being able to activate the nuclear factor-κB inflammation pathway,[20] our current data suggest that excessive levels of extracellular trypsin enhance the sensitivity of acinar cells to ferroptosis, but not apoptosis and necroptosis. As an oxidative stress–dependent cell death,[68] ferroptosis is characterized by necrotic changes, such as plasma rupture and the release of damage-associated molecular patterns (eg, HMGB1).[69,70] Different from intracellular HMGB1, which scavenges cellular damage, extracellular HMGB1 is a mediator of sterile inflammation in mouse models of pancreatitis.[71] Unlike apoptosis and necrosis, ferroptosis can be initiated without the contribution of caspases and MLKL.[26,27] Unrestricted lipid peroxidation and the abnormal lysosomal degradation pathways that are observed commonly in pancreatitis all are implicated in inducing ferroptosis in vitro and in vivo.[69] Here, we documented that the presence of excessive trypsin dramatically increases the susceptibility of acinar cells to various ferroptosis activators.

Our study highlights a new mechanism by which PSMD4-dependent proteasomal degradation of GPX4 promotes ferroptosis in acinar cells. The lipid hydroperoxidase GPX4 has the unique ability to detoxify lipid hydroperoxide into harmless alcohol and water, thereby preventing ferroptotic damage.[72–74] The degradation of GPX4 appears to be a common response to ferroptosis activators.[42,48,75] In contrast to selective autophagy, which mediates GPX4 degradation in ferroptotic cancer cells,[48] our current study suggests that the activation of the ubiquitin-proteasome system is responsible for GPX4 degradation in ferroptotic acinar cells. Although the core E3 ubiquitin ligase responsible for GPX4 degradation remains elusive, PSMD4 (a proteasome ubiquitin receptor) plays a significant role in mediating GPX4 degradation to induce ferroptosis.

Figure 4. (***See previous page***). **Olanzapine is a new ferroptosis inhibitor in acinar cells.** (*A*) Chemical structures of 5 potential ferroptosis inhibitors. (*B*) Analysis of cell death in 266-6 cells after treatment with cerulein (100 nmol/L), L-arginine (5 mg/mL), alcohol (50 mmol/L), erastin (2 μmol/L), and RSL3 (500 nmol/L) in the absence or presence of trypsin (500 ng/mL), olanzapine (10 μmol/L), idebenone (10 μmol/L), telmisartan (10 μmol/L), nisoldipine (10 μmol/L), and azelnidipine (10 μmol/L) for 24 hours. Data are shown in a heat map as the mean of 3 biologically independent samples. (*C*) Analysis of cell death in 266-6 cells after treatment with cerulein (100 nmol/L)/trypsin (500 ng/mL) in the absence or presence of olanzapine (10 μmol/L), risperidone (10 μmol/L), SB204741 (10 μmol/L), and SB242084 (10 μmol/L) for 24 hours. Data are presented as means ± SD; n = 3 biologically independent samples; 2-way analysis of variance (ANOVA) with the Tukey multiple comparisons test on all pairwise combinations. (*D*) Analysis of mRNA expression in indicated gene knockdown 266-6 cells. Data are presented as means ± SD; n = 3 biologically independent samples. (*E*) Analysis of cell death in indicated gene knockdown 266-6 cells after treatment with cerulein (100 nmol/L)/trypsin (500 ng/mL) for 24 hours. Data are presented as means ± SD; n = 3 biologically independent samples; 2-way ANOVA with the Tukey multiple comparisons test on all pairwise combinations. (*F*) Scavenging DPPH free radical activity of indicated drugs. Data are presented as means ± SD; n = 3 biologically independent samples; 1-way ANOVA test on all pairwise combinations. (*G–I*) Analysis of (G) lipid peroxidation, (*H*) C20:4, and (*I*) C22:4 in 266-6 cells after treatment with cerulein (100 nmol/L)/trypsin (500 ng/mL) in the absence or presence of ferrostatin-1 (1 μmol/L), olanzapine (10 μmol/L), risperidone (10 μmol/L), SB204741 (10 μmol/L), and SB242084 (10 μmol/L) for 24 hours. Data are presented as means ± SD; n = 3 biologically independent samples; 1-way ANOVA test on all pairwise combinations. (*J*) Analysis of GPX4 protein expression in 266-6 cells after treatment with cerulein (100 nmol/L)/trypsin (500 ng/mL) in the absence or presence of olanzapine (10 μmol/L) for 24 hours. Semiquantitative data are presented as means ± SD; n = 3 biologically independent samples; 1-way ANOVA test on all pairwise combinations. ACTB, actin beta; Ctrl, control; sh, shRNA.

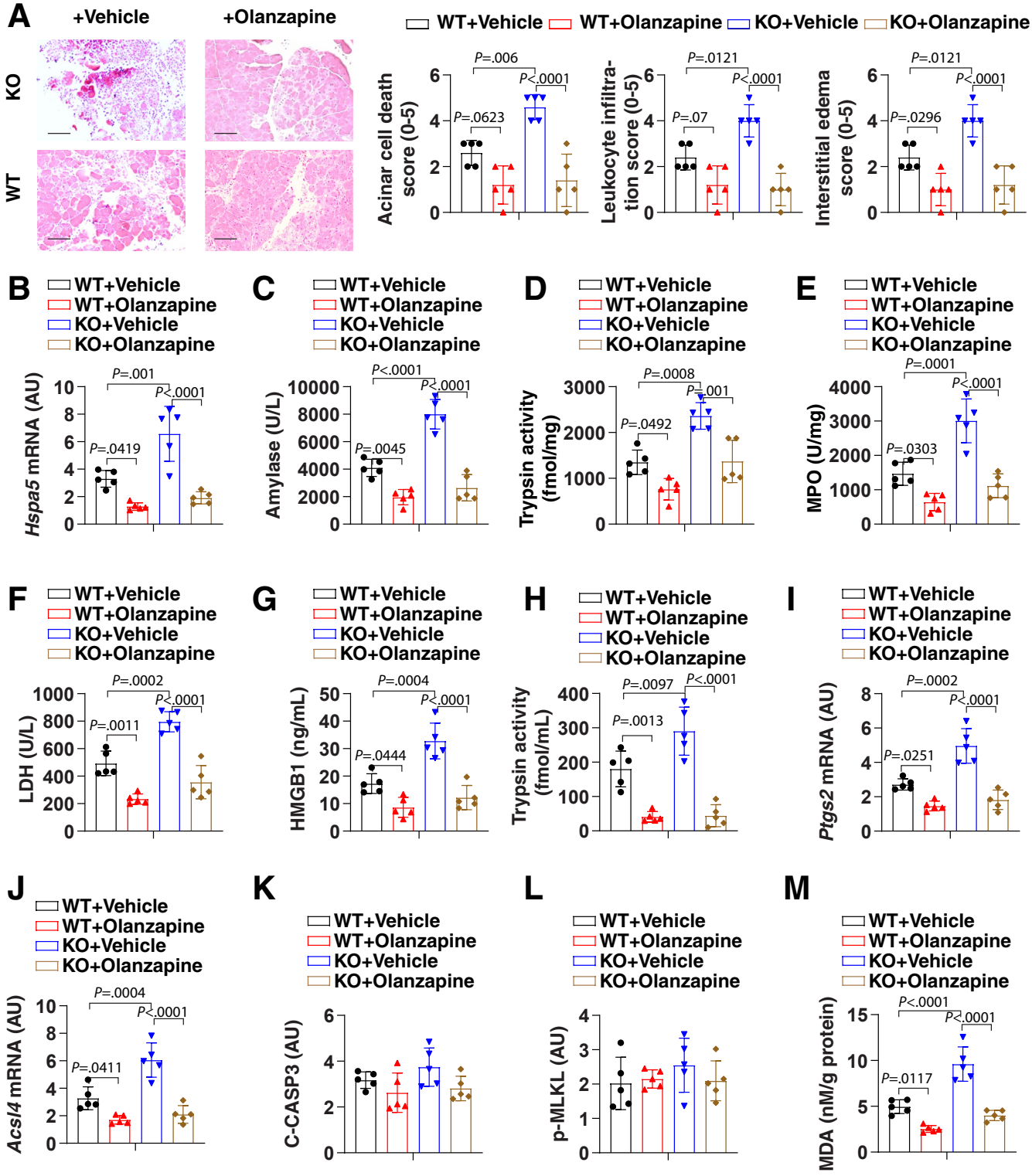

Figure 5. Ferroptotic damage increases the severity of acute pancreatitis in mice. (*A*) Representative images of pancreatic histology in cerulein-induced pancreatitis in *Gpx4* WT and KO mice with or without olanzapine (5 mg/kg) treatment. Histologic scores. for acinar cell death, leukocyte infiltration, and edema at 12 hours after the last cerulein treatment were evaluated. Data are presented as means ± SD; n = 5 mice/group; 1-way analysis of variance (ANOVA) test on all pairwise combinations. Bar=100 μm (*B–L*) In parallel, (*B*) pancreatic *Hspa5* mRNA, (*C*) serum amylase, (*D*) pancreatic trypsin activity, (*E*) pancreatic MPO activity, (*F*) serum LDH, (*G*) serum HMGB1, (*H*) serum trypsin activity, (*I*) pancreatic *Ptgs2* mRNA, (*J*) pancreatic *Acsl4* mRNA, (*K*) pancreatic cleaved caspase-3 (C-CASP3), (*L*) pancreatic p-MLKL, and (*M*) pancreatic MDA at 12 hours after the last cerulein treatment were assayed. Data are presented as means ± SD; n = 5 mice/group; 1-way ANOVA test on all pairwise combinations.

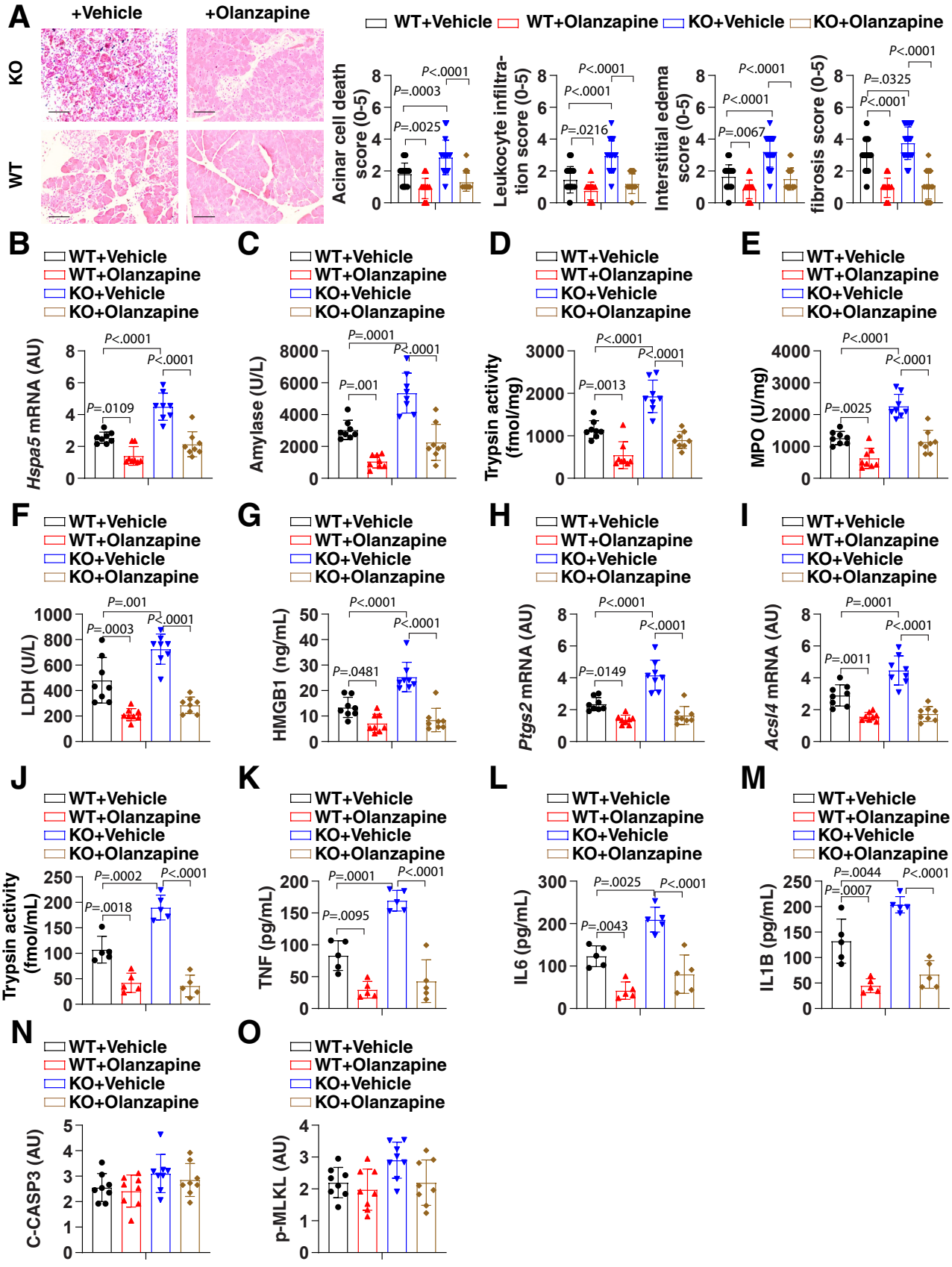
A
+Vehicle
+Olanzapine
KO
WT
WT+Vehicle
WT+Olanzapine
KO+Vehicle
KO+Olanzapine
Acinar cell death score (0-5)
Leukocyte infiltration score (0-5)
Interstitial edema score (0-5)
fibrosis score (0-5)
B
Hspa5 mRNA (AU)
C
Amylase (U/L)
D
Trypsin activity (fmol/mg)
E
MPO (U/mg)
F
LDH (U/L)
G
HMGB1 (ng/mL)
H
Ptgs2 mRNA (AU)
I
Acsl4 mRNA (AU)
J
Trypsin activity (fmol/mL)
K
TNF (pg/mL)
L
IL6 (pg/mL)
M
IL1B (pg/mL)
N
C-CASP3 (AU)
O
p-MLKL (AU)

Consequently, blocking PSMD4-dependent GPX4 degradation inhibits trypsin-enhanced ferroptosis in acinar cells. In fact, administration of the proteasome inhibitor MG132 prevents the onset of acute pancreatitis in mice,[76,77] supporting the notion that the proteasomal degradation pathway is one of the therapeutic targets of pancreatitis.

The depletion of pancreatic *Gpx4* does not affect the normal development and physiological function of the pancreas, but exacerbates acute or chronic pancreatitis caused by pathologic (eg, cerulein) or clinically relevant stressors (eg, alcohol).[32] We showed that pancreatic *Gpx4* depletion triggers a feed-forward loop between lipid peroxidation and trypsin activation during experimental pancreatitis. In contrast to the pancreas, the depletion of *Gpx4* in other, nonpancreatic tissues or cells, such as the kidney or T cells, may cause spontaneous tissue damage in a ferroptosis-dependent manner.[72,73] In addition, the loss of *Gpx4* in myeloid cells increased susceptibility to bacterial infections through lipid peroxidation–dependent pyroptosis, rather than ferroptosis.[78] Therefore, GPX4 has physiological or pathologic functions that differ according to tissue type or stimulation.[28,78–80] It is worth noting that a recent study showed that genetic ablation of the antioxidant enzyme peroxiredoxin 1 in the pancreas prevents cerulein-induced pancreatitis through a redox-independent mechanism.[81] Further understanding of the overlap and different functions of antioxidant enzymes in pancreatitis may establish new strategies to limit sterile inflammation.

In summary, we provide evidence that trypsin-mediated sensitization of pancreatic acinar cells to ferroptosis may be targeted for the prevention and treatment of pancreatitis in mice. An unbiased drug screening campaign identified olanzapine (a drug used to treat certain psychiatric conditions, such as schizophrenia, bipolar disorder, and depression[82]) as a novel ferroptosis inhibitor that prevents pancreatitis in mice. These findings may accelerate translational research on the suppression of ferroptotic damage in human pancreatitis.

Materials and Methods

Reagents

Erastin (S7242), RSL3 (S8155), ferrostatin-1 (S7243), liproxstatin-1 (S7699), Z-VAD-FMK (S7023), necrosulfonamide (S8251), staurosporine (S1421), CCT137690 (S2744), olanzapine (S2493), idebenone (S2605), telmisartan (S1738), nisoldipine (S1748), azelnidipine (S3053), and risperidone (S1615) were obtained from Selleck Chemicals (Houston, TX). Cerulein (C9026), L-arginine (A5006), alcohol (PHR1373), 2-mercaptoethanol (M6250), trypsin (T1426), soybean trypsin inhibitor (650357), SB204741 (S0693), and SB242084 (5.06417) were obtained from Sigma-Aldrich (Burlington, MA). Dimethyl sulfoxide (472301; Sigma-Aldrich) was used to prepare the stock solution of most drugs. The final concentration of dimethyl sulfoxide in the drug working solution in the cells was less than 0.01%. In addition, 0.01% dimethyl sulfoxide was used as a vehicle control in the corresponding cell culture assays.

The antibodies to PSMD4 (sc-398033) and actin beta (ACTB, sc-8432) were obtained from Santa Cruz Biotechnology (Dallas, TX). The antibodies to GPX4 (ab125066) and SLC7A11 (ab175186) were obtained from Abcam (Cambridge, MA). The antibodies to ferritin heavy chain 1 (3998) and ARNTL (14020) were obtained from Abcam. The antibodies to SLC40A1 (NBP1-21502) and apoptosis inducing factor mitochondria-associated 2 (H00084883-D01P) were obtained from NOVUS (Saint Charles, MO).

Pancreatitis Models

The protocol for animal use was reviewed and approved by our institutional animal care and use committees. Pancreatic-specific *Gpx4* knockout mice were produced and identified in our laboratory by crossing floxed *Gpx4* (a gift from Dr Qitao Ran, University of Texas Health, San Antonio, TX) and *Pdx1-Cre* (014647; The Jackson Laboratory, Bar Harbor, ME) transgenic mice (C57BL/6J background) as previously described.[32] Mouse were kept under standard pathogen-free conditions with an artificial 12-hour light/dark cycle (lights on: 8:00 AM) and constant 50%–60% humidity. Mice were allowed access to tap water and free (ad libitum) access to standard laboratory chow during the experimental period.

For cerulein-induced acute pancreatitis, male mice (age, 8–10 wk) received 7 hourly intraperitoneal injections of 50 μg/kg cerulein in sterile saline.[83] Olanzapine was repeatedly administered orally by gavage at a dose of 5 mg/kg to mice at 3 and 12 hours after the first cerulein injection, while controls were treated by oral administration with vehicle (smooth peanut butter).[84] The parameters of acute pancreatitis were assessed 12 hours after the last cerulein treatment. For the induction of chronic pancreatitis, male mice (age, 8–10 wk) were fed a Lieber–DeCarli ethanol (5% vol/vol) liquid diet for 4 weeks (F1258; Bio-Serv, Flemington, NJ).[85] In parallel, olanzapine was administered orally by gavage at a dose of 5 mg/kg to mice (3 times per week, over 4 weeks), while controls were treated by oral administration with vehicle. The parameters of chronic pancreatitis were assessed in mice 4 weeks after feeding them the Lieber–DeCarli ethanol liquid diet.

Figure 6. (***See previous page***). **Ferroptotic damage increases the severity of chronic pancreatitis in mice.** (*A*) Representative images of pancreatic histology in Lieber–DeCarli alcoholic liquid diet–induced pancreatitis in *Gpx4* WT and KO mice with or without olanzapine (5 mg/kg) treatment. Histologic scores for acinar cell death, leukocyte infiltration, edema, and fibrosis at 4 weeks after Lieber–DeCarli alcoholic liquid diet were evaluated. Data are presented as means ± SD; n = 20 mice/group; 1-way ANOVA test on all pairwise combinations. Bar=100 μm (*B–O*) In parallel, (*B*) pancreatic *Hspa5* mRNA, (*C*) serum amylase, (*D*) pancreatic trypsin activity, (*E*) pancreatic MPO activity, (*F*) serum LDH, (*G*) serum HMGB1, (*H*) pancreatic *Ptgs2* mRNA, (*I*) pancreatic *Acsl4* mRNA, (*J*) serum trypsin activity, (*K*) serum tumor necrosis factor (TNF), (*L*) serum IL6, (*M*) serum IL1B, (*N*) pancreatic cleaved caspase-3 (C-CASP3), and (*O*) pancreatic p-MLKL at 4 weeks after Lieber–DeCarli alcoholic liquid diet were assayed. Data are presented as means ± SD; n = 5–8 mice/group; 1-way ANOVA test on all pairwise combinations.

Animals were killed at the indicated time by CO_2 asphyxia, and a blood sample and tissue were collected. Serum was collected further immediately after centrifugation at 10,000 × *g* for 5 minutes at 4°C. Tissue samples were collected, snap-frozen in liquid nitrogen, and stored at -80°C. Formalin-fixed pancreas samples were processed, and 5-μm–thick paraffin sections were stained with H&E for histologic analysis. Pancreatitis was scored according to a revised scoring standard,[86] with an independent pathologist evaluating histologic scores for acinar cell death, leukocyte infiltration, or edema in a blind manner. Histologic images were acquired using an EVOS FL Auto Cell Imaging System (Thermo Fisher Scientific, Pittsburgh, PA).

Cell Culture

The 266-6 (CRL-2151) cell line was obtained from the American Type Culture Collection and cultured in Dulbecco's modified Eagle medium (11995073; Thermo Fisher Scientific) supplemented with 10% heat-inactivated fetal bovine serum (A3840001; Thermo Fisher Scientific) and 1% penicillin and streptomycin (15070-063; Thermo Fisher Scientific) at 37°C, 95% humidity, and 5% CO_2. Primary mouse acinar cells were cultured as described below. Briefly, the pancreas from male C57BL/6J mice (age, 8–10 wk) was removed and minced for 5 minutes in Hank's balanced salt solution (H8264; Sigma-Aldrich) plus 0.1% bovine serum albumin (05470; Sigma-Aldrich) and 10 mmol/L HEPES (PHG0001; Sigma-Aldrich). After washing, the pancreatic segments were incubated in 10 mL collagenase IA solution (Hank's balanced salt solution 1× containing 10 mmol/L HEPES, 200 U/mL of collagenase IA [C9891; Sigma-Aldrich], and 0.25 mg/mL of trypsin inhibitor) for 20–30 minutes at 37°C. The solution containing collagenase then was removed and replaced with Dulbecco's modified Eagle medium supplemented with 1% penicillin and streptomycin, 10% fetal bovine serum, 0.25 mg/mL trypsin inhibitor, and 25 ng/mL recombinant mouse epidermal growth factor (E5160; Sigma-Aldrich) at 37°C, 95% humidity, and 5% CO_2. Cell line identity was validated by short tandem repeat profiling, and routine mycoplasma testing was negative for contamination.

Western Blot Analysis

Cells were lysed 3 times with 1× cell lysis buffer (9803; Cell Signaling Technology, Danvers, MA) containing protease inhibitor cocktail (P8340; Sigma-Aldrich) on ice for 10 minutes. Protein was quantified using the bicinchoninic acid assay (23225; Thermo Fisher Scientific) and 20–30 μg of each sample was resolved on 4%–12% Criterion XT Bis-Tris gels (3450124; Bio-Rad) in XT MES running buffer (1610789; Bio-Rad) and transferred to polyvinylidene difluoride membranes (1620233; Bio-Rad) using the Trans-Blot Turbo Transfer Pack and System (1704150; Bio-Rad). Membranes were blocked with Tris-buffered saline with 0.1% Tween 20 detergent (TBST) containing 5% nonfat milk (9999; Cell Signaling Technology) for 1 hour and incubated overnight at 4°C with various primary antibodies (1:500–1:1000). After 3 washes in TBST, membranes were incubated with goat anti-rabbit or anti-mouse IgG horseradish peroxidase–conjugated secondary antibody (1:1000, 7074 or 7076; Cell Signaling Technology) at room temperature for 1 hour. After being washed with TBST, the signals were visualized using enhanced chemiluminescence (32106; Thermo Fisher Scientific) and then visualized and analyzed with a ChemiDoc Touch Imaging System (Bio-Rad).

Immunoprecipitation Analysis

Cells were lysed at 4°C in pre-cold radioimmunoprecipitation assay lysis buffer (9806; Cell Signaling Technology) and cell lysates were cleared by brief centrifugation (12,000 × *g* for 10 minutes).[87] Concentrations of proteins in the supernatant were determined by bicinchoninic acid assay (23225; Thermo Fisher Scientific). Before immunoprecipitation, samples containing equal amounts of proteins were precleared with protein A agarose beads (9863; Cell Signaling Technology) at 4°C for 3 hours and subsequently incubated with irrelevant IgG or specific antibodies (5 μg/mL) in the presence of protein A agarose beads overnight at 4°C with gentle shaking. After incubation, protein A agarose beads were washed extensively with phosphate-buffered saline and proteins were eluted by boiling in 2 × Laemmli sample buffer (161-0737; Bio-Rad) before sodium dodecyl sulfate–polyacrylamide gel electrophoresis.

Cytotoxicity Assays

A Countess II FL Automated Cell Counter (Thermo Fisher Scientific) was used to assay the percentage of dead cells after cell staining with 0.4% trypan blue solution (T10282; Thermo Fisher Scientific). Cells were suspended as single cells in buffered saline. If cell clumps (especially primary acinar cells) were seen in the sample tube, these samples were filtered with nylon mesh to remove aggregates. Samples then were prepared by adding 10 μL of cell suspension to 10 μL of 0.4% trypan blue stain.

Food and Drug Administration–Approved Drug Screening

The Food and Drug Administration–approved drug library was obtained from Selleck Chemicals (L1300). The 266-6 cells were seeded into 96-well plates and then treated with cerulein (100 nmol/L)/trypsin (500 ng/mL) in the absence or presence of a drug (10 μmol/L) for 24 hours. Subsequently, 100 μL fresh medium was added to cells containing 10 μL Cell Counting Kit-8 (CCK-8) solutions (CK04; Dojindo Laboratories, Rockville, MD) and incubated for 2 hours (37°C, 5% CO_2). Cell viability was measured at 450-nm absorbance using a microplate reader (Cytation 5 Cell Imaging Multi-Mode Reader, Winooski, VA). The effects of top drug candidates on cerulein-/trypsin-induced cell death in 266-6 cells were assayed further using a Countess II FL Automated Cell Counter.

Quantitative Real-Time Polymerase Chain Reaction Assay

Total RNA was extracted and purified from cultured cells using the RNeasy Plus Mini Kit (74136; QIAGEN, Germantown, MD). First-strand complementary DNA (cDNA) was synthesized from 1 μg RNA using the iScript cDNA Synthesis Kit (1708890; Bio-Rad). Briefly, 20-μL reactions were prepared by combining 4 μL iScript Select reaction mix, 2 μL gene-specific enhancer solution, 1 μL reverse transcriptase, 1 μL gene-specific assay pool (20×, 2 μmol/L), and 12 μL RNA diluted in RNase-free water. Then cDNA from various cell samples was amplified by real-time qPCR with specific primers using a CFX96 Touch Real-Time PCR Detection System (Bio-Rad) with CFX Manager software 2.0 (Bio-Rad). The data were normalized to Rna18S and the fold change was calculated via the 2-ΔΔCt method. The relative concentrations of mRNA were expressed in arbitrary units based on the untreated group, which was assigned a value of 1. The predesigned primers were obtained from OriGene Technologies (Rockville, Maryland, USA).

RNAi and Gene Transfection

Psmd4 shRNA (GTACCGGGAAACTAGCTAAACGCCTTAACTCGAGTTAAGGCGTTTAGCTAGTTTCTTTTTTG), Gpx4 shRNA (CCGGCCGGCTACAACGTCAAGTTTGCTCGAGCAAACTTGACGTTGTAGCCGGTTTTTG), Htr2a shRNA (CCGGCCCACTGGTATATACGTTGTTCTCGAGAACAACGTATATACCAGTGGGTTTTT), Htr2b shRNA (CCGGGCGGTGATAATACCCACCATTCTCGAGAATGGTGGGTATTATCACCGCTTTTT), Htr2c shRNA (CCGGGCTTCCAAAGTCCTTGGCATTCTCGAGAATGCCAAGGACTTTGGAAGCTTTTT), and Acsl4 shRNA (CCGGGCAGAAGATTATTGTGTTGATCTCGAGATCAACACAATAATCTTCTGCTTTTT) were obtained from Sigma-Aldrich. Psmd4 cDNA (MC200621) was obtained from OriGene Technologies. The shRNA or indicated cDNA were transfected into cells using Lipofectamine 3000 (L3000-015; Invitrogen, Pittsburgh, PA) or Lipofectamine RNAiMAX (13778030; Invitrogen) when cells were at approximately 60%–70% confluence. Puromycin (ant-pr-1; InvivoGen, San Diego, CA) was used to generate stable knockdown cell lines. The efficiency of RNAi and gene transfection was verified by reverse-transcription PCR or Western blot.

Enzyme-Linked Immunosorbent Assay Analysis

The concentrations or activity of amylase (ab102523; Abcam), MPO (EMMPO; Thermo Fisher Scientific), trypsin (ab102531; Abcam), 8-hydroxy-2-deoxyguanosine (K4160; BioVision, Milpitas, CA), HMGB1 (326054329; Sino-Test Corporation, Tokyo, Japan), LDH (ab102526; Abcam), cleaved-caspase3 (DYC835-2; R&D Systems, Minneapolis, MN), p-MLKL (PEL-MLKL-S345-1; RayBiotech Life, Norcross, GA), MDA (ab118970; Abcam), iron (MAK025; Sigma-Aldrich), GSH (CS0260; Sigma-Aldrich), CoQ10 (MBS7233016; MyBioSource, San Diego, CA), tumor necrosis factor (BMS607-3; Thermo Fisher Scientific), IL6 (BMS603-2; Thermo Fisher Scientific), and IL1B (BMS6002; Thermo Fisher Scientific) in the indicated samples were measured using enzyme-linked immunosorbent assay kits according to the manufacturer's guidelines. Data were normalized to protein or DNA concentration.

Lipid Peroxidation Assay

BODIPY 581/591 C11 probe (D3861; Thermo Fisher Scientific) was used to detect lipid peroxidation according to the manufacturer's instructions. Briefly, cells were incubated with BODIPY 581/591 C11 at a final concentration of 5 μmol/L for 30 minutes at 37°C and washed 3 times with phosphate-buffered saline. Oxidation of the polyunsaturated butadienyl portion of the dye resulted in a shift of the fluorescence emission peak from approximately 590 nm to approximately 510 nm, which was measured in a Bio-Tek fluorescence microplate reader (Winooski, VA).

DPPH Radical Scavenging Assay

The free radical scavenging ability of the indicated drugs was tested by a DPPH radical scavenging assay. DPPH produces purple/violet in methanol solution and fades to yellow in the presence of antioxidants. Briefly, a reaction mixture containing 2.4 mL of 0.1 mmol/L DPPH in methanol and 1.6 mL of tested drugs (1 μmol/L ferrostatin-1, 10 μmol/L olanzapine, 10 μmol/L risperidone, 10 μmol/L SB204741, and 10 μmol/L SB242084) was incubated in a dark environment at 25°C for 30 minutes. The optical absorbance at 517 nm of the mixture was measured in triplicate after centrifugation. The DPPH radical scavenging activity was expressed in arbitrary units based on the untreated group, which was assigned a value of 1. Ferrostatin-1 was used as a positive control.

Liquid Chromatography with Tandem Mass Spectrometry Method for Lipid Analysis

Reverse-phase chromatography was selected for LC separation using the CSH C18 column (1.7 μm, 2.1 mm × 100 mm; Waters Corp, Milford, MD). The lipid extracts were re-dissolved in 200 μL 90% isopropanol/acetonitrile, centrifuged at 14,000 × g for 15 minutes, and finally 3 μL of sample was injected. Solvent A was acetonitrile–water (6:4, vol/vol) with 0.1% formic acid and 0.1 mmol/L ammonium formate and solvent B was acetonitrile–isopropanol (1:9, vol/vol) with 0.1% formic acid and 0.1 mmol/L ammonium formate. The initial mobile phase was 30% solvent B at a flow rate of 300 μL/min. It was held for 2 minutes, and then increased linearly to 100% solvent B in 23 minutes, followed by equilibrating at 5% solvent B for 10 minutes.

Mass spectra were acquired with Q-Exactive Plus (Pittsburgh, PA) in positive and negative mode, respectively. Electrospray ionization (ESI) parameters were optimized and preset for all measurements as follows: source temperature, 300°C; capillary temperature, 350°C; ion spray voltage, 3000 V; S-lens RF level, 50%; and the scan range of the instruments, 200–1800 m/z. LipidSearch Software 5.0 (Thermo Fisher Scientific) was used to identify lipid species based on MS/MS data. The control group was assigned a value of 1, and the treatment group then was calculated relative to the control group.

Statistical Analysis

Data are presented as means ± SD except where otherwise indicated. GraphPad Prism 8.4.3 (San Diego, CA) was used to collect and analyze data. A *t* test was used to compare the means of 2 groups. A 1-way or 2-way analysis of variance with the Tukey multiple comparisons test was used for comparison among the different groups. A *P* value less than .05 was considered statistically significant. We did not exclude samples or animals. For every figure in this article, statistical tests are justified when appropriate. All data meet the assumptions of the tests (eg, normal distribution).

References

1. Beck IT, Kahn DS, Solymar J, McKenna RD, Zylberszac B. The role of pancreatic enzymes in the pathogenesis of acute pancreatitis. III. Comparison of the pathologic and biochemical changes in the canine pancreas to intraductal injection with bile and with trypsin. Gastroenterology 1964;46:531–542.
2. Hegyi E, Sahin-Toth M. Genetic risk in chronic pancreatitis: the trypsin-dependent pathway. Dig Dis Sci 2017; 62:1692–1701.
3. Ji B, Logsdon CD. Digesting new information about the role of trypsin in pancreatitis. Gastroenterology 2011; 141:1972–1975.
4. Neoptolemos JP, Kemppainen EA, Mayer JM, Fitzpatrick JM, Raraty MG, Slavin J, Beger HG, Hietaranta AJ, Puolakkainen PA. Early prediction of severity in acute pancreatitis by urinary trypsinogen activation peptide: a multicentre study. Lancet 2000; 355:1955–1960.
5. Gudgeon AM, Heath DI, Hurley P, Jehanli A, Patel G, Wilson C, Shenkin A, Austen BM, Imrie CW, Hermon-Taylor J. Trypsinogen activation peptides assay in the early prediction of severity of acute pancreatitis. Lancet 1990;335:4–8.
6. Whitcomb DC, Gorry MC, Preston RA, Furey W, Sossenheimer MJ, Ulrich CD, Martin SP, Gates LK Jr, Amann ST, Toskes PP, Liddle R, McGrath K, Uomo G, Post JC, Ehrlich GD. Hereditary pancreatitis is caused by a mutation in the cationic trypsinogen gene. Nat Genet 1996;14:141–145.
7. Teich N, Rosendahl J, Toth M, Mossner J, Sahin-Toth M. Mutations of human cationic trypsinogen (PRSS1) and chronic pancreatitis. Hum Mutat 2006;27:721–730.
8. Nemeth BC, Sahin-Toth M. Human cationic trypsinogen (PRSS1) variants and chronic pancreatitis. Am J Physiol Gastrointest Liver Physiol 2014;306:G466–G473.
9. Witt H, Luck W, Hennies HC, Classen M, Kage A, Lass U, Landt O, Becker M. Mutations in the gene encoding the serine protease inhibitor, Kazal type 1 are associated with chronic pancreatitis. Nat Genet 2000;25:213–216.
10. Pfutzer RH, Barmada MM, Brunskill AP, Finch R, Hart PS, Neoptolemos J, Furey WF, Whitcomb DC. SPINK1/PSTI polymorphisms act as disease modifiers in familial and idiopathic chronic pancreatitis. Gastroenterology 2000;119:615–623.
11. Muller N, Sarantitis I, Rouanet M, de Mestier L, Halloran C, Greenhalf W, Ferec C, Masson E, Ruszniewski P, Levy P, Neoptolemos J, Buscail L, Rebours V. Natural history of SPINK1 germline mutation related-pancreatitis. EBioMedicine 2019;48:581–591.
12. Chandak GR, Idris MM, Reddy DN, Mani KR, Bhaskar S, Rao GV, Singh L. Absence of PRSS1 mutations and association of SPINK1 trypsin inhibitor mutations in hereditary and non-hereditary chronic pancreatitis. Gut 2004;53:723–728.
13. Huang H, Swidnicka-Siergiejko AK, Daniluk J, Gaiser S, Yao Y, Peng L, Zhang Y, Liu Y, Dong M, Zhan X, Wang H, Bi Y, Li Z, Ji B, Logsdon CD. Transgenic expression of PRSS1(R122H) sensitizes mice to pancreatitis. Gastroenterology 2020;158:1072–1082 e7.
14. Gui F, Zhang Y, Wan J, Zhan X, Yao Y, Li Y, Haddock AN, Shi J, Guo J, Chen J, Zhu X, Edenfield BH, Zhuang L, Hu C, Wang Y, Mukhopadhyay D, Radisky ES, Zhang L, Lugea A, Pandol SJ, Bi Y, Ji B. Trypsin activity governs increased susceptibility to pancreatitis in mice expressing human PRSS1R122H. J Clin Invest 2020;130: 189–202.
15. Jancso Z, Sahin-Toth M. Mutation that promotes activation of trypsinogen increases severity of secretagogue-induced pancreatitis in mice. Gastroenterology 2020;158:1083–1094.
16. Rakonczay Z Jr, Hegyi P, Takacs T, McCarroll J, Saluja AK. The role of NF-kappaB activation in the pathogenesis of acute pancreatitis. Gut 2008; 57:259–267.
17. Huang H, Liu Y, Daniluk J, Gaiser S, Chu J, Wang H, Li ZS, Logsdon CD, Ji B. Activation of nuclear factor-kappaB in acinar cells increases the severity of pancreatitis in mice. Gastroenterology 2013;144:202–210.
18. Zhan X, Wan J, Zhang G, Song L, Gui F, Zhang Y, Li Y, Guo J, Dawra RK, Saluja AK, Haddock AN, Zhang L, Bi Y, Ji B. Elevated intracellular trypsin exacerbates acute pancreatitis and chronic pancreatitis in mice. Am J Physiol Gastrointest Liver Physiol 2019;316:G816–G825.
19. Gaiser S, Daniluk J, Liu Y, Tsou L, Chu J, Lee W, Longnecker DS, Logsdon CD, Ji B. Intracellular activation of trypsinogen in transgenic mice induces acute but not chronic pancreatitis. Gut 2011;60:1379–1388.
20. Ji B, Gaiser S, Chen X, Ernst SA, Logsdon CD. Intracellular trypsin induces pancreatic acinar cell death but not NF-kappaB activation. J Biol Chem 2009; 284:17488–17498.
21. Sendler M, Lerch MM. The complex role of trypsin in pancreatitis. Gastroenterology 2020;158:822–826.
22. Kang R, Lotze MT, Zeh HJ, Billiar TR, Tang D. Cell death and DAMPs in acute pancreatitis. Mol Med 2014; 20:466–477.
23. Criddle DN, Gerasimenko JV, Baumgartner HK, Jaffar M, Voronina S, Sutton R, Petersen OH, Gerasimenko OV. Calcium signalling and pancreatic cell death: apoptosis or necrosis? Cell Death Differ 2007;14:1285–1294.
24. Petrov MS, Shanbhag S, Chakraborty M, Phillips AR, Windsor JA. Organ failure and infection of pancreatic necrosis as determinants of mortality in patients with

acute pancreatitis. Gastroenterology 2010;139:813–820.
25. Bakker OJ, van Santvoort HC, Besselink MG, van der Harst E, Hofker HS, Gooszen HG. Dutch Pancreatitis Study Group. Prevention, detection, and management of infected necrosis in severe acute pancreatitis. Curr Gastroenterol Rep 2009;11:104–110.
26. Chen X, Li J, Kang R, Klionsky DJ, Tang D. Ferroptosis: machinery and regulation. Autophagy 2021; 17:2054–2081.
27. Tang D, Chen X, Kang R, Kroemer G. Ferroptosis: molecular mechanisms and health implications. Cell Res 2021;31:107–125.
28. Chen X, Kang R, Kroemer G, Tang D. Ferroptosis in infection, inflammation, and immunity. J Exp Med 2021; 218:e20210518.
29. Kimita W, Petrov MS. Iron metabolism and the exocrine pancreas. Clin Chim Acta 2020;511:167–176.
30. Ma D, Li C, Jiang P, Jiang Y, Wang J, Zhang D. Inhibition of ferroptosis attenuates acute kidney injury in rats with severe acute pancreatitis. Dig Dis Sci 2020;66:483–492.
31. Liu Y, Wang Y, Liu J, Kang R, Tang D. The circadian clock protects against ferroptosis-induced sterile inflammation. Biochem Biophys Res Commun 2020; 525:620–625.
32. Dai E, Han L, Liu J, Xie Y, Zeh HJ, Kang R, Bai L, Tang D. Ferroptotic damage promotes pancreatic tumorigenesis through a TMEM173/STING-dependent DNA sensor pathway. Nat Commun 2020;11:6339.
33. Meher S, Mishra TS, Sasmal PK, Rath S, Sharma R, Rout B, Sahu MK. Role of biomarkers in diagnosis and prognostic evaluation of acute pancreatitis. J Biomark 2015;2015:519534.
34. Artigas JM, Garcia ME, Faure MR, Gimeno AM. Serum trypsin levels in acute pancreatic and non-pancreatic abdominal conditions. Postgrad Med J 1981; 57:219–222.
35. Cristina Oliveira de Lima V, Piuvezam G, Leal Lima Maciel B, Heloneida de Araujo Morais A. Trypsin inhibitors: promising candidate satietogenic proteins as complementary treatment for obesity and metabolic disorders? J Enzyme Inhib Med Chem 2019;34:405–419.
36. Draper HH, Hadley M. Malondialdehyde determination as index of lipid peroxidation. Methods Enzymol 1990; 186:421–431.
37. Dixon SJ, Lemberg KM, Lamprecht MR, Skouta R, Zaitsev EM, Gleason CE, Patel DN, Bauer AJ, Cantley AM, Yang WS, Morrison B 3rd, Stockwell BR. Ferroptosis: an iron-dependent form of nonapoptotic cell death. Cell 2012;149:1060–1072.
38. Malsy M, Bitzinger D, Graf B, Bundscherer A. Staurosporine induces apoptosis in pancreatic carcinoma cells PaTu 8988t and Panc-1 via the intrinsic signaling pathway. Eur J Med Res 2019;24:5.
39. Xie Y, Zhu S, Zhong M, Yang M, Sun X, Liu J, Kroemer G, Lotze M, Zeh HJ 3rd, Kang R, Tang D. Inhibition of aurora kinase a induces necroptosis in pancreatic carcinoma. Gastroenterology 2017;153:1429–1443 e5.
40. Yang Y, Luo M, Zhang K, Zhang J, Gao T, Connell DO, Yao F, Mu C, Cai B, Shang Y, Chen W. Nedd4 ubiquitylates VDAC2/3 to suppress erastin-induced ferroptosis in melanoma. Nat Commun 2020;11:433.
41. Wang Y, Liu Y, Liu J, Kang R, Tang D. NEDD4L-mediated LTF protein degradation limits ferroptosis. Biochem Biophys Res Commun 2020;531:581–587.
42. Yang L, Chen X, Yang Q, Chen J, Huang Q, Yao L, Yan D, Wu J, Zhang P, Tang D, Zhong N, Liu J. Broad spectrum deubiquitinase inhibition induces both apoptosis and ferroptosis in cancer cells. Front Oncol 2020;10:949.
43. Chen X, Yu C, Kang R, Kroemer G, Tang D. Cellular degradation systems in ferroptosis. Cell Death Differ 2021;28:1135–1148.
44. Lin Z, Liu J, Kang R, Yang M, Tang D. Lipid metabolism in ferroptosis. Adv Biol (Weinh) 2021;5:e2100396.
45. Kagan VE, Mao G, Qu F, Angeli JP, Doll S, Croix CS, Dar HH, Liu B, Tyurin VA, Ritov VB, Kapralov AA, Amoscato AA, Jiang J, Anthonymuthu T, Mohammadyani D, Yang Q, Proneth B, Klein-Seetharaman J, Watkins S, Bahar I, Greenberger J, Mallampalli RK, Stockwell BR, Tyurina YY, Conrad M, Bayir H. Oxidized arachidonic and adrenic PEs navigate cells to ferroptosis. Nat Chem Biol 2017;13:81–90.
46. Yang WS, SriRamaratnam R, Welsch ME, Shimada K, Skouta R, Viswanathan VS, Cheah JH, Clemons PA, Shamji AF, Clish CB, Brown LM, Girotti AW, Cornish VW, Schreiber SL, Stockwell BR. Regulation of ferroptotic cancer cell death by GPX4. Cell 2014;156:317–331.
47. Xie Y, Hou W, Song X, Yu Y, Huang J, Sun X, Kang R, Tang D. Ferroptosis: process and function. Cell Death Differ 2016;23:369–379.
48. Wu Z, Geng Y, Lu X, Shi Y, Wu G, Zhang M, Shan B, Pan H, Yuan J. Chaperone-mediated autophagy is involved in the execution of ferroptosis. Proc Natl Acad Sci U S A 2019;116:2996–3005.
49. Hou W, Xie Y, Song X, Sun X, Lotze MT, Zeh HJ 3rd, Kang R, Tang D. Autophagy promotes ferroptosis by degradation of ferritin. Autophagy 2016;12:1425–1428.
50. Yang M, Chen P, Liu J, Zhu S, Kroemer G, Klionsky DJ, Lotze MT, Zeh HJ, Kang R, Tang D. Clockophagy is a novel selective autophagy process favoring ferroptosis. Sci Adv 2019;5:eaaw2238.
51. Li J, Liu J, Xu Y, et al. Tumor heterogeneity in autophagy-dependent ferroptosis. Autophagy 2021. https://doi.org/10.1080/15548627.2021.1872241, Epub ahead of print.
52. Liu J, Kuang F, Kroemer G, Klionsky DJ, Kang R, Tang D. Autophagy-dependent ferroptosis: machinery and regulation. Cell Chem Biol 2020;27:420–435.
53. Doll S, Freitas FP, Shah R, Aldrovandi M, da Silva MC, Ingold I, Grocin AG, Xavier da Silva TN, Panzilius E, Scheel CH, Mourao A, Buday K, Sato M, Wanninger J, Vignane T, Mohana V, Rehberg M, Flatley A, Schepers A, Kurz A, White D, Sauer M, Sattler M, Tate EW, Schmitz W, Schulze A, O'Donnell V, Proneth B, Popowicz GM, Pratt DA, Angeli JPF, Conrad M. FSP1 is a glutathione-independent ferroptosis suppressor. Nature 2019;575:693–698.

54. Bersuker K, Hendricks JM, Li Z, Magtanong L, Ford B, Tang PH, Roberts MA, Tong B, Maimone TJ, Zoncu R, Bassik MC, Nomura DK, Dixon SJ, Olzmann JA. The CoQ oxidoreductase FSP1 acts parallel to GPX4 to inhibit ferroptosis. Nature 2019;575:688–692.
55. Dai E, Zhang W, Cong D, Kang R, Wang J, Tang D. AIFM2 blocks ferroptosis independent of ubiquinol metabolism. Biochem Biophys Res Commun 2020; 523:966–971.
56. Chen X, Kang R, Kroemer G, Tang D. Broadening horizons: the role of ferroptosis in cancer. Nat Rev Clin Oncol 2021;18:280–296.
57. Yuan H, Li X, Zhang X, Kang R, Tang D. Identification of ACSL4 as a biomarker and contributor of ferroptosis. Biochem Biophys Res Commun 2016;478:1338–1343.
58. Doll S, Proneth B, Tyurina YY, Panzilius E, Kobayashi S, Ingold I, Irmler M, Beckers J, Aichler M, Walch A, Prokisch H, Trumbach D, Mao G, Qu F, Bayir H, Fullekrug J, Scheel CH, Wurst W, Schick JA, Kagan VE, Angeli JP, Conrad M. ACSL4 dictates ferroptosis sensitivity by shaping cellular lipid composition. Nat Chem Biol 2017;13:91–98.
59. Irving HM, Samokhvalov AV, Rehm J. Alcohol as a risk factor for pancreatitis. A systematic review and meta-analysis. JOP 2009;10:387–392.
60. Hirota M, Ohmuraya M, Baba H. The role of trypsin, trypsin inhibitor, and trypsin receptor in the onset and aggravation of pancreatitis. J Gastroenterol 2006; 41:832–836.
61. Halangk W, Lerch MM, Brandt-Nedelev B, Roth W, Ruthenbuerger M, Reinheckel T, Domschke W, Lippert H, Peters C, Deussing J. Role of cathepsin B in intracellular trypsinogen activation and the onset of acute pancreatitis. J Clin Invest 2000;106:773–781.
62. Sendler M, Weiss FU, Golchert J, Homuth G, van den Brandt C, Mahajan UM, Partecke LI, Doring P, Gukovsky I, Gukovskaya AS, Wagh PR, Lerch MM, Mayerle J. Cathepsin B-mediated activation of trypsinogen in endocytosing macrophages increases severity of pancreatitis in mice. Gastroenterology 2018;154:704–718 e10.
63. Kuang F, Liu J, Li C, Kang R, Tang D. Cathepsin B is a mediator of organelle-specific initiation of ferroptosis. Biochem Biophys Res Commun 2020;533:1464–1469.
64. Gao H, Bai Y, Jia Y, Zhao Y, Kang R, Tang D, Dai E. Ferroptosis is a lysosomal cell death process. Biochem Biophys Res Commun 2018;503:1550–1556.
65. Archer H, Jura N, Keller J, Jacobson M, Bar-Sagi D. A mouse model of hereditary pancreatitis generated by transgenic expression of R122H trypsinogen. Gastroenterology 2006;131:1844–1855.
66. Geisz A, Sahin-Toth M. A preclinical model of chronic pancreatitis driven by trypsinogen autoactivation. Nat Commun 2018;9:5033.
67. Selig L, Sack U, Gaiser S, Kloppel G, Savkovic V, Mossner J, Keim V, Bodeker H. Characterisation of a transgenic mouse expressing R122H human cationic trypsinogen. BMC Gastroenterol 2006;6:30.
68. Kuang F, Liu J, Tang D, Kang R. Oxidative damage and antioxidant defense in ferroptosis. Front Cell Dev Biol 2020;8:586578.
69. Tang D, Chen X, Kang R, Kroemer G. Ferroptosis: molecular mechanisms and health implications. Cell Res 2021;31:107–125.
70. Chen X, Comish PB, Tang D, Kang R. Characteristics and biomarkers of ferroptosis. Front Cell Dev Biol 2021; 9:637162.
71. Kang R, Zhang Q, Hou W, Yan Z, Chen R, Bonaroti J, Bansal P, Billiar TR, Tsung A, Wang Q, Bartlett DL, Whitcomb DC, Chang EB, Zhu X, Wang H, Lu B, Tracey KJ, Cao L, Fan XG, Lotze MT, Zeh HJ 3rd, Tang D. Intracellular Hmgb1 inhibits inflammatory nucleosome release and limits acute pancreatitis in mice. Gastroenterology 2014;146:1097–1107.
72. Friedmann Angeli JP, Schneider M, Proneth B, Tyurina YY, Tyurin VA, Hammond VJ, Herbach N, Aichler M, Walch A, Eggenhofer E, Basavarajappa D, Radmark O, Kobayashi S, Seibt T, Beck H, Neff F, Esposito I, Wanke R, Forster H, Yefremova O, Heinrichmeyer M, Bornkamm GW, Geissler EK, Thomas SB, Stockwell BR, O'Donnell VB, Kagan VE, Schick JA, Conrad M. Inactivation of the ferroptosis regulator Gpx4 triggers acute renal failure in mice. Nat Cell Biol 2014;16:1180–1191.
73. Matsushita M, Freigang S, Schneider C, Conrad M, Bornkamm GW, Kopf M. T cell lipid peroxidation induces ferroptosis and prevents immunity to infection. J Exp Med 2015;212:555–568.
74. Mayr L, Grabherr F, Schwarzler J, Reitmeier I, Sommer F, Gehmacher T, Niederreiter L, He GW, Ruder B, Kunz KTR, Tymoszuk P, Hilbe R, Haschka D, Feistritzer C, Gerner RR, Enrich B, Przysiecki N, Seifert M, Keller MA, Oberhuber G, Sprung S, Ran Q, Koch R, Effenberger M, Tancevski I, Zoller H, Moschen AR, Weiss G, Becker C, Rosenstiel P, Kaser A, Tilg H, Adolph TE. Dietary lipids fuel GPX4-restricted enteritis resembling Crohn's disease. Nat Commun 2020;11:1775.
75. Liu Y, Wang Y, Liu J, Kang R, Tang D. Interplay between MTOR and GPX4 signaling modulates autophagy-dependent ferroptotic cancer cell death. Cancer Gene Ther 2021;28:55–63.
76. Letoha T, Somlai C, Takacs T, Szabolcs A, Rakonczay Z Jr, Jarmay K, Szalontai T, Varga I, Kaszaki J, Boros I, Duda E, Hackler L, Kurucz I, Penke B. The proteasome inhibitor MG132 protects against acute pancreatitis. Free Radic Biol Med 2005;39:1142–1151.
77. Letoha T, Feher LZ, Pecze L, Somlai C, Varga I, Kaszaki J, Toth G, Vizler C, Tiszlavicz L, Takacs T. Therapeutic proteasome inhibition in experimental acute pancreatitis. World J Gastroenterol 2007;13:4452–4457.
78. Kang R, Zeng L, Zhu S, Xie Y, Liu J, Wen Q, Cao L, Xie M, Ran Q, Kroemer G, Wang H, Billiar TR, Jiang J, Tang D. Lipid peroxidation drives gasdermin D-mediated pyroptosis in lethal polymicrobial sepsis. Cell Host Microbe 2018;24:97–108 e4.
79. Canli O, Alankus YB, Grootjans S, Vegi N, Hultner L, Hoppe PS, Schroeder T, Vandenabeele P, Bornkamm GW, Greten FR. Glutathione peroxidase 4 prevents necroptosis in mouse erythroid precursors. Blood 2016;127:139–148.
80. Ran Q, Gu M, Van Remmen H, Strong R, Roberts JL, Richardson A. Glutathione peroxidase 4 protects cortical

neurons from oxidative injury and amyloid toxicity. J Neurosci Res 2006;84:202–208.
81. Buckens H, Pirenne S, Achouri Y, Baldan J, Dahou H, Bouwens L, Lemaigre FP, Jacquemin P, Assi M. Peroxiredoxin-I sustains inflammation during pancreatitis. Cell Mol Gastroenterol Hepatol 2021;12:741–743.
82. Meftah AM, Deckler E, Citrome L, Kantrowitz JT. New discoveries for an old drug: a review of recent olanzapine research. Postgrad Med 2020;132:80–90.
83. Mareninova OA, Hermann K, French SW, O'Konski MS, Pandol SJ, Webster P, Erickson AH, Katunuma N, Gorelick FS, Gukovsky I, Gukovskaya AS. Impaired autophagic flux mediates acinar cell vacuole formation and trypsinogen activation in rodent models of acute pancreatitis. J Clin Invest 2009;119:3340–3355.
84. Cope MB, Nagy TR, Fernandez JR, Geary N, Casey DE, Allison DB. Antipsychotic drug-induced weight gain: development of an animal model. Int J Obes (Lond) 2005; 29:607–614.
85. Orekhova A, Geisz A, Sahin-Toth M. Ethanol feeding accelerates pancreatitis progression in CPA1 N256K mutant mice. Am J Physiol Gastrointest Liver Physiol 2020;318:G694–G704.
86. Schmidt J, Rattner DW, Lewandrowski K, Compton CC, Mandavilli U, Knoefel WT, Warshaw AL. A better model of acute pancreatitis for evaluating therapy. Ann Surg 1992;215:44–56.
87. Tang D, Kang R, Livesey KM, Cheh CW, Farkas A, Loughran P, Hoppe G, Bianchi ME, Tracey KJ, Zeh HJ 3rd, Lotze MT. Endogenous HMGB1 regulates autophagy. J Cell Biol 2010;190:881–892.

Received July 5, 2021. Accepted September 15, 2021.

Correspondence
Address correspondence to: Daolin Tang, MD, Department of Surgery, University of Texas Southwestern Medical Center, 5323 Harry Hines Boulevard, Dallas, Texas 75390 e-mail: daolin.tang@utsouthwestern.edu; or Jun Huang, MD, Department of Orthopaedics, The 2nd Xiangya Hospital, Central South University, Changsha 410011, China; fax: (86) 731-85295999 e-mail: 505447@csu.edu.cn.

Acknowledgments
The authors thank Dave Primm (Department of Surgery, University of Texas Southwestern Medical Center) for critical reading of the manuscript.

CRediT Authorship Contributions
Ke Liu (Data curation: Lead)
Jiao Liu (Data curation: Lead)
Borong Zou (Data curation: Equal)
Changfeng Li (Data curation: Equal)
Herbert Zeh (Writing – review & editing: Equal)
Rui Kang (Data curation: Equal; Methodology: Equal)
Guido Kroemer (Writing – review & editing: Lead)
Jun Huang (Conceptualization: Lead; Formal analysis: Lead; Writing – original draft: Equal)
Daolin Tang, MD, PhD (Conceptualization: Lead; Data curation: Lead; Formal analysis: Lead; Investigation: Lead; Methodology: Lead; Project administration: Lead; Supervision: Lead; Writing – original draft: Lead; Writing – review & editing: Lead)

Conflicts of interest
The authors disclose no conflicts.

Funding
This work was supported by the American Cancer Society grant RSG-16-014-01 (D.T.), and by the National Natural Science Foundation of China grants 81872323 and 82073299 (C.L.).